European MSc in Marine Environment and Resources
UPV/EHU–SOTON–UB-ULg

Erasmus Mundus

REF: 2013-0237

Master Thesis Project

Comparative analysis of the phytoplankton chlorophyll to carbon ratio in eight marine ecosystem models

Author
Caroline Jacques

Supervisors
Dr. Christoph Voelker
Dr. Judith Hauck

Marine BioGeoScience Department
Alfred Wegener Institute, Germany

Plentzia (UPV/EHU), September 2015

université de BORDEAUX

University of Southampton

eman ta zabal zazu
Universidad del País Vasco
Euskal Herriko Unibertsitatea

Université de Liège

European MSc in Marine Environment and Resources

UPV/EHU–SOTON–UB-ULg

Erasmus Mundus

REF: 2013-0237

Dr
as teaching staff of the MER Master of the University of

CERTIFIES:

That the research work entitled
COMPARATIVE ANALYSIS OF THE PHYTOPLANKTON CHLOROPHYLL TO CARBON RATIO IN EIGHT MARINE ECOSYSTEM MODELS

has been carried out by
CAROLINE JACQUES

in
MARINE BIOGEOSCIENCE DEPARTMENT
ALFRED WEGENER INSTITUTE, GERMANY

under the supervision of
Dr CHRISTOPH VOELKER & Dr JUDITH HAUCK

from the
ALFRED WEGENER INSTITUTE, GERMANY

in order to achieve 30 ECTS as a part of the MER Master program.

In September 2015

Signed: Supervisor

université de BORDEAUX

UNIVERSITY OF Southampton

Universidad del Pais Vasco Euskal Herriko Unibertsitatea

Université de Liège

Acknowledgements

I would like to thank my supervisors, Christoph Voelker and Judith Hauck, to have helped me during these seven months at the Alfred Wegener Institute. Thank you for your availability, your wise advice and your kindness.

A special thank you to Dieter Wolf-Gladrow to have welcomed me in the Marine BioGeoScience department.

I also would like to thank the MER consortium to have given me the opportunity to achieve this master around Europe. It was both a scientific and personal adventure.

I am so grateful to have met such wonderful persons during this master. We have travelled and evolved together for the last two years. I cherish our friendships so much.

Thank you to my amazing family and lovely grandparents for believing in me. Your support is more than precious to me.

Thank you to Ayrton, to have followed me around Europe, to have given us a chance, to have been so supportive and comforting. I am so lucky to have you by my side.

Thank you to my sister Julie for being there whenever I needed it. You know me better than anyone and could find the right words to reassure me. I hope I can return the favour one day. You are wonderful.

I would not be doing this master if it was not for my parents. I do not know how to express my gratitude. Thirteen years I have wanted to become an oceanographer and here I am. Thank you for giving me this extraordinary chance. Thank you for your unconditional support and your love.

Abstract

Chlorophyll *a* is often used as a proxy to estimate marine phytoplankton biomass given its optical properties that can be easily measured both *in situ* and remotely. The Chl:C ratio which is used to convert from chlorophyll to biomass, is, however, not constant in phytoplankton. It depends on temperature, light and nutrients, and is assumed to be regulated by the cells to maximise the growth rate under limiting environmental conditions. This process, called acclimation, increases the chlorophyll content under low light and decreases it under nutrient limitation. The Geider model that allows for dynamic Chl:C ratios is now included in an increasing number of marine ecosystem models. However, the ratios are seldomly validated and their effect on net primary production estimations from chlorophyll data is still highly uncertain. The aim of this study is to compare the Chl:C ratio in eight model simulations from the MARine Ecosystem Model Intercomparison Project (MAREMIP) and/or the Coupled Model Intercomparison Project Phase 5 (CMIP5), i.e. REcoM2, TOPAZ, MEM, NOBM, PlankTOM5.3, BEC, CNRM-PISCES and IPSL-PISCES. We focus on the annual climatology of the ratio in surface waters for the period 2000-2005. To assess the ability of these simulations to represent the chlorophyll field, we first compare model outputs with satellite observations. It appears that the main patterns in chlorophyll distribution are modelled quite well in the open ocean, but not in coastal areas, partly due to the coarse resolution of these model runs. The core analysis of this study consists in investigating the reasons behind the discrepancies in the Chl:C ratio among models. We highlight that models have different ways of dealing with this ratio: MEM uses a constant ratio, the ratio in NOBM is only light-dependent, and the remaining models allow for a variable ratio. Nevertheless, they all agree on the fact that the slope of the linear regression between phytoplankton carbon and chlorophyll is a number smaller than 1. In the group of models considering a variable ratio, the annual climatology of the Chl:C ratio simulated by REcoM2 substantially differs. We demonstrate that the Chl degradation rate is probably too high in this model run and that the minimum tolerated values of the ratio are too low. Eventually, an interesting feature about REcoM2 is that it can handle unbalanced growth conditions. Some of the other models are only valid under the hypothesis of balanced growth, which rarely happens in natural environments. We hope this present study brings some enlightenment on the variability of the phytoplankton Chl:C ratio and will contribute to improve our estimations of primary production and by this means, future climate projections.

Key words: Phytoplankton · Chlorophyll-to-carbon ratio · Acclimation · Marine ecosystem models · MAREMIP · CMIP · Light limitation · Nutrient limitation · Growth rate

Résumé

La chlorophylle *a* est souvent utilisée comme proxy pour évaluer la biomasse du phytoplancton marin grâce à ses propriétés optiques qui peuvent être mesurées facilement à la fois *in situ* et par satellite. Le ratio Chl:C qui est utilisé pour convertir la chlorophylle en biomasse n'est cependant pas constant dans le phytoplancton. Il dépend de la température, de la lumière et des nutriments, et serait régulé par les celllules pour maximiser leur taux de croissance dans des conditions environnementales limitantes. Ce processus, appelé acclimatation, augmente le contenu en chlorophylle lorsque la luminosité est faible et le diminue lorsque la concentration en nutriments est insuffisante. Le modèle établi par Geider permet d'obtenir un ratio Chl:C dynamique et est maintenant intégré dans un nombre croissant de modèles d'écosystèmes marins. Cependant, les ratios sont rarement validés et leur impact sur les estimations de la production primaire nette à partir de données de chlorophylle est toujours très incertain. L'objectif de cette étude est de comparer le ratio Chl:C dans huit simulations de modèles faisant partie du MARine Ecosystem Model Intercomparison Project (MAREMIP) et/ou du Coupled Model Intercomparison Project Phase 5 (CMIP5), à savoir REcoM2, TOPAZ, MEM, NOBM, PlankTOM5.3, BEC, CNRM-PISCES et IPSL-PISCES. Nous nous focalisons sur la climatologie annuelle du ratio dans les eaux de surface entre 2000 et 2005. Pour évaluer la capacité de ces simulations à représenter la chlorophylle, nous comparons tout d'abord les sorties générées par les modèles avec les observations satellites. Il apparaît que les principales structures inhérentes à la distribution de la chlorophylle sont bien représentées par les modèles en haute mer, mais pas dans les zones côtières, notamment à cause de la résolution grossière de ces simulations. L'analyse centrale de cette étude réside dans l'investigation des raisons qui pourraient expliquer les différences dans le ratio Chl:C entre les modèles. Nous mettons en évidence que les modèles considèrent ce ratio de façons différentes: MEM utilise un ratio constant, le ratio dans NOBM dépend uniquement de la lumière et les autres modèles permettent au ratio de varier. Tous ces modèles s'accordent sur le fait que la pente de la régression linéaire entre le contenu en carbon du phytoplancton et le contenu en chlorophylle est un nombre inférieur à 1. Parmi les modèles qui considèrent un ratio variable, la climatologie annuelle du ratio Chl:C simulée par REcoM2 diffère notablement. Nous démontrons que le taux de dégradation de la chlorophylle est probablement trop élevé dans cette simulation de REcoM2 et que les valeurs minimales tolérées pour le ratio sont trop basses. Finalement, une caractéristique intéressante de REcoM2 est que ce modèle est capable de gérer des conditions de croissance en non-équilibre. Certains autres modèles sont valides uniquement dans l'hypothèse que la croissance est en équilibre, ce qui arrive rarement dans la nature. Nous espérons que la présente étude apportera des éclaircissements sur l'origine de la variabilité du ratio Chl:C du phytoplancton et qu'elle contribuera à améliorer les estimations de la production océanique primaire et ainsi, les projections climatiques.

Mots-clés: Phytoplancton · Ratio chlorophylle-carbon · Acclimatation · Modèles d'ecosystèmes marins · MAREMIP · CMIP · Manque de lumière · Manque de nutriments

Table of contents

Part I

Introduction

1 Context

Over the last decades, the carbon cycle has been the centre of growing attention. In a context of global warming, it has indeed become crucial to better understand the sources and sinks of carbon as well as the main protagonists of the complex equilibrium between oceans, atmosphere, biosphere and geosphere. Phytoplankton, these microscopic photosynthetic organisms living in surface oceans, play a particularly determinant role in biogeochemical cycles. Aside from producing half of the oxygen we breathe, they capture carbon dioxide to synthesize organic matter. The export of this organic matter to the deep ocean represents a major sink of atmospheric carbon. Improving our knowledge on this fundamental compartment of the carbon cycle will allow to constrain the uncertainties associated with future climate projections and provide more reliable information to policy makers so that, hopefully, adequate actions can be taken to reduce anthropogenic greenhouse gas emissions.

As *in situ* measurements can be expensive and quite difficult to implement on a large scale, ocean biogeochemical models have proven to be powerful tools in improving our understanding of marine ecosystem dynamics. Their number and complexity have greatly increased over the last twenty years and it has become necessary to evaluate their performance and compare their outputs. This effort has been started by the "Ocean-Carbon Cycle Model Intercomparison Project (OCMIP)" with a focus on biogeochemistry, and continued by the "Coupled Model Intercomparison Project Phase 5 (CMIP5)", which is more climate-oriented, and by the "MARine Ecosystem Model Intercomparison Project (MAREMIP)", focused on ecosystem dynamics. These projects aim for model improvement in order to answer important questions regarding biogeochemical cycles.

Thanks to the development of satellite imagery, ocean surface concentrations in the photosynthetic pigment chlorophyll *a* (Chl) can now be calculated continuously from backscattered radiations in the blue and green wavelengths. Rapidly, Chl has become one of the reference proxies for the assessment of marine phytoplankton carbon (C) biomass. The conversion of Chl estimations into C biomass is made using a Chl:C ratio. However, the Chl:C ratio is not constant among phytoplankton species and strongly depends on environmental conditions, i.e. temperature, light and nutrients (Geider et al., 1998). Indeed, phytoplankton can adapt their cellular composition to maximise their growth rate under limiting conditions and to minimise the potential damages arising from high irradiance (Geider et al., 1998). This process, called acclimation, affects our estimations of primary production and therefore increases the uncertainty surrounding the carbon cycle. Most MAREMIP and CMIP models now allow for a dynamic Chl:C ratio, based on the Geider

model, however the ratios are seldomly validated and their impact on net primary production estimations is still not well understood. It is therefore essential to conduct thorough studies on the parameterization of this ratio in simulations to improve model estimations of primary productivity.

2 Objectives

The aim of this master thesis is to contribute to this joint effort in evaluating model performances. In order to do so, we study eight model simulations from MAREMIP and/or CMIP5, i.e. REcoM2, TOPAZ, MEM, NOBM, PlankTOM5.3, BEC, CNRM-PISCES and IPSL-PISCES. This work is articulated around three key analyses. The first step consists in assessing the ability of the models to simulate Chl concentrations in surface oceans by confronting them with satellite observations. The purpose of this section is to obtain an early qualitative overview of the strengths and limitations of models.

Then, in the central analysis of this master thesis, we focus on the phytoplankton Chl:C ratio in model simulations. We are particularly interested in comparing the global pattern of the ratio in surface oceans and identifying the main regions of divergence. We also try to understand the reasons behind discrepancies in model outputs by having a look at their structural equations.

Eventually, we focus on REcoM2, as this model behaves quite differently regarding the distribution of the Chl:C ratio in surface waters. With this section, we want to push the thinking a little further and begin an analysis of the processes that drive Chl:C ratio variability in models.

Part II
State of the art

1 Phytoplankton and marine primary production

As microscopic as they can be, phytoplankton are nevertheless the base of essentially all life in marine ecosystems. These drifting organisms, distributed among at least eight different phyla, cover a range of sizes going from less than 1 to more than 100 microns (Chavez et al., 2011). Cyanobacteria, encompassing all prokaryotic phytoplankton, are maybe more abundant than eukaryotic phytoplankton, but the latter ones have a greater influence on marine ecosystems as they drive most of the organic matter flux to the deep ocean (Falkowski et al., 2004). The three groups of eukaryotic phytoplankton responsible for most of this export are diatoms, dinoflagellates and coccolithophores (Falkowski et al., 2004).

Unlike their taxonomist colleagues, modellers are more interested in plankton functions than in their classification. They have therefore defined Plankton Functional Types (PFTs) to group plankton according to their specific biogeochemical role in marine ecosystems. Le Quéré et al. (2005) consider ten key PFTs, six of them being phytoplankton PFTs. Two straightforward examples are silicifiers, whose worthy representatives are diatoms, and calcifiers, mostly represented by coccolithophorids. This functional classification allows for finer description of biogeochemical processes. The definition of each class of PFT and their associated physiological parameters can be found in Le Quéré et al. (2005). Taking into consideration the six phytoplankton PFTs considerably increases the amount of physiological data required, this is why most models limit their number of phytoplankton PFTs to two or three.

Regardless of their function, all phytoplanktonic organisms live in the euphotic zone where they can capture the light required to carry out photosynthesis, and through this process, convert solar energy into chemical energy. From water and carbon dioxide, oxygen and carbohydrates are formed, following the simplified reaction:

$$6\,CO_2 + 6\,H_2O \xrightarrow{\text{Solar energy}} C_6H_{12}O_6 + 6\,O_2$$

Synthesis of organic compounds from inorganic material is termed primary production. Although phytoplankton account only for less than 1% of the total photosynthetic biomass, they are responsible for the net primary production (NPP) of about 50 petagrams of carbon per year, which is equivalent to terrestrial environments (Field, 1998). They are also the source of about half the oxygen we breathe. By regulating atmospheric oxygen and carbon dioxide concentrations, they play a major role in global biogeochemical cycles and climate (Chavez et al., 2011).

This essential reaction, supporting the whole marine foodweb, would not be possible without chlorophyll, a photosynthetic green pigment that acts as a photoreceptor. Several types of chlorophyll molecules exist, differing in their absorption spectrum, but chlorophyll *a* is the only one that is systematically present in photosynthetic organisms. For convenience, we will refer to chlorophyll *a* as Chl later in this work. As phytoplankton carbon (C) is difficult to estimate, Chl measurements have been chosen preferentially to assess phytoplankton biomass (Chavez et al., 2011). The most common methods used in laboratories and *in situ* sampling are spectrophotometry, high performance liquid chromatography (HPLC), and fluorometry, but all these techniques have a limited spatial coverage. As mentioned in the introduction, global Chl estimations are now routinely provided by satellites, then an algorithm is subsequently applied to determine surface phytoplankton biomass. This algorithm requires the utilization of a Chl:C ratio, which is generally set constant. However, it has become widely accepted that the relationship between Chl and C is not linear but depends on species and environmental factors such as light intensity, temperature and nutrient availability (Geider, 1987). This topic will be further developed in the following section.

2 Phytoplankton growth

Apart from light, carbon dioxide and water, phytoplankton also need nutrients to achieve photosynthesis. The major macronutrients are nitrogen (N) and phosphorus (P), and in the case of diatoms, silicium (Si). Some particularly important micronutrients are trace metals such as iron (Fe), zinc (Zn), manganese (Mn), nickel (Ni), copper (Cu), cobalt (Co) and cadmium (Cd). These nutrients are taken up in a very selective way to synthesize organic matter. Redfield (1958) studied the proportion of the different elements and noticed that phytoplankton cellular composition follows on average a constant ratio of 106C:16N:1P. This ratio was later extended to iron and is now widely used as a conversion factor in oceanography even though deviations from this ratio have been documented (e.g. Geider and La Roche, 2002).

If all the macro- and micro-nutrients required for phytoplankton development are available, and if the light and temperature conditions are favourable, the growth rate will be maximal. Unfortunately, this rarely happens in natural environments, and phytoplankton growth is therefore often limited. To describe how growth is impacted by the limited availability of a specific nutrient, it is common to use a Michaelis-Menten function:

$$N_{lim} = \frac{[N]}{[N] + K_N} \tag{1}$$

where N is the nutrient and K is the half saturation constant of this nutrient. As several studies on phytoplankton nutrient uptake demonstrated the shortcomings associated with

the use of Michaelis-Menten kinetics, Aksnes and Egge (1991) published a more physiological description of the nutrient uptake rate (V) based on uptake site characteristics and nutrient affinity:

$$V = \frac{nAvS}{1 + hAvS} \tag{2}$$

where n is the cellular number of uptake sites, A is the uptake site area, v is the mass transfer coefficient, S is the substrate concentration and h is time required to handle one nutrient ion. The authors highlight that the Michaelis-Menten model becomes therefore a special case of their model in which the parameters n, h, A and v are constant. This means that the Michaelis-Menten model is only valid if the time scale considered is small enough to keep these parameters unaltered (Aksnes and Egge, 1991).

Once the limitation has been computed for each nutrient, Liebig's Law of the Minimum is often used to infer the growth under multiple limitations (Liebig, 1840). This law was initially developed in agriculture to describe the dependency of the yield on the most limiting nutrient. It was then transposed in oceanography where it changed to become that the scarcest nutrient limits phytoplankton growth (de Baar, 1994). However, some authors argue that in natural environments, and particularly surface oceans, several nutrients can be simultaneously scarce, leading to colimitation (Saito et al., 2008). Based on laboratory studies, Saito et al. (2008) identify three distinct types of colimitation. Their full descriptions and mathematical formulations can be found in Saito et al. (2008).

To describe the influence of temperature, Eppley (1972) developed an empirical function based on a compilation of growth rates at different temperatures. In this function, the maximum growth rate is proportional to an exponential function of the temperature:

$$\mu_{max} \propto e^{k_{Eppley} \cdot T} \tag{3}$$

where μ_{max} is the maximum growth rate, the Eppley constant k_{Eppley} is equal to 0.063 $(°C)^{-1}$ and T is the temperature in °C.

Eventually, to describe how light can limit phytoplankton growth, it is common to use a Poisson function of irradiance $f(I)$ (Geider et al., 1998):

$$f(I) = 1 - \exp\left(\frac{-\alpha^{Chl}\theta^{C}E_0}{P^{C}_{max}}\right) \tag{4}$$

where α^{Chl} is the Chl-specific initial slope of the photosynthesis-light curve, θ^{C} is the phytoplankton Chl:C ratio, E_0 is the incident irradiance and P^{C}_{max} is the maximum rate of photosynthesis. It is important to stress that this function is influenced by the Chl:C ratio.

In vitro measurements on phytoplankton growth are generally conducted in an experimental system called chemostat. This continuous culture system consists in a flow of fertilized medium pumped into a culture chamber at a fixed rate and a simultaneous outflow of excess culture (Hoskisson and Hobbs, 2005). By this process, the chemostat provides a constant environment. The first advantage of this method is that it allows to control exactly the physico-chemical conditions within the culture chamber, and therefore increases the reproducibility of the experiment. The second advantage is that it leads to balanced growth as the growth rate is kept constant. In natural environments, balanced growth is encountered only when the rates of change of the different cellular pools are equal, which means that carbon fixation, nutrient assimilation and light utilization have to be strictly coupled (Geider et al., 1998). However, highly variable environmental conditions often prevent achieving this coupling (Geider et al., 1998).

3 Impact of environmental conditions on the chlorophyll to carbon ratio

These limiting environmental conditions do not only affect growth, they also lead to modifications in phytoplankton cellular composition. There is an extensive literature on the topic, which would be impossible to review in depth here, so we will only describe some key studies. Back in the 1940s, the first experiments were conducted proving that changes in light intensities could affect the photosynthetic characteristics of the green algae *Chlorella pyrenoidosa* (Myers, 1946). Ever since then, researchers have tried to identify phytoplankton responses to changing light. Beale and Appleman (1971) found out that chlorophyll concentration in *Chlorella* cells increases when light limits the growth and decreases when light is not limiting. Based on laboratory studies, Shuter (1979) built a growth model whose particularity is that phytoplankton cellular carbon is divided in four compartments. Under a specific combination of light intensity, nutrient availability and temperature, growth is balanced and therefore a unique carbon allocation between these four compartments exists. Thanks to this model, the authors could show that changes in cellular composition induced by environmental conditions occur in order to maximise the growth rate (Shuter, 1979). Falkowski and Owens (1980) studied the influence of light on the size and number of photosynthetic units in *Skeletonema costatum* and *Dunaliella tertiolecta*. They noticed that the two organisms differ in their responses: *S. costatum* showed a change in the size of its photosynthetic units whereas in *D. tertiolecta*, the number of photosynthetic units was changing, meaning that species have different ways of dealing with light limitation. Laws and Bannister (1980) studied the impact of light and nutrient limitation on *Thalassiossira fluvialis* growth rate. They argue that, as phytoplankton are able to grow over a large range of environmental conditions without changing their cellular composition too much, metabolic mechanisms regulating nutrient uptake should exist in order to maintain balanced growth (Laws and Bannister, 1980). To understand these mechanisms, they grew *T.*

fluvialis under nitrate, ammonium, then phosphate and eventually light limitation. At each step, they measured the Chl:C and N:C ratios. The results obtained for the Chl:C ratio are presented in Figure 1. It clearly appears that the Chl:C ratio decreases with increasing growth rate under light limitation and increases with increasing growth rate under nutrient limitations. This experiment demonstrates that phytoplankton are able to modify their internal composition to adapt themselves to limiting conditions. Cullen (1982) called for caution when interpreting Chl vertical profiles and in particular Deep Chlorophyll Maxima (DCM) that can arise from different mechanisms, among which physiological adaptation of the C:Chl ratio. The author also mentioned that *in vivo* fluorescence per unit of Chl is highly variable and depends especially on light, species composition and phytoplankton nutritional state (Cullen, 1982). Cullen and Lewis (1988) studied the kinetics of photoadaptation and suggested that photoadaptative parameters could be used to determine the rate of vertical mixing. If there is a vertical gradient in phytoplankton adaptation to light in the surface mixed layer, it means that the time scale for photoadaptation is shorter than the vertical mixing, whereas if no gradient appears, then mixing is faster than photoadaptation (Cullen and Lewis, 1988). The authors identified parameters changing over a time scale of about an hour, i.e. the initial slope of the photosynthesis-irradiance curve and the *in vivo* fluorescence, and parameters requiring much longer time scales to adapt from low to high light, i.e. the chemical composition and the photosynthetic capacity (Cullen and Lewis, 1988). The concept of photoacclimation was mentioned by Falkowski and LaRoche (1991). The authors use the term "acclimation" for physiological changes that they distinguish from evolutional processes for which they use the term "adaptation" (Falkowski and LaRoche, 1991). Photoacclimation can occur at the physiological, cellular and morphological level. For the purpose of this work, we will focus on the varying chlorophyll concentration.

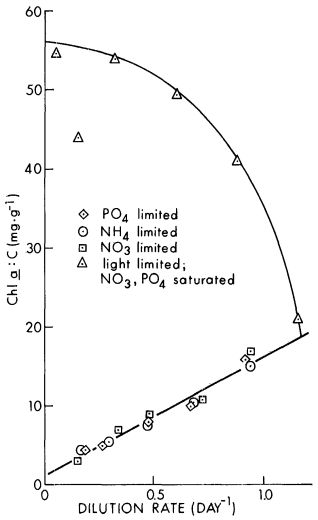

Figure 1: Dependence of the Chl:C ratio on the dilution rate under light and nutrient limitations, from Laws and Bannister (1980). A higher dilution rate is equivalent to a higher growth rate

4 Phytoplankton acclimation in models

Many models were successful in describing the resource-response relationship for one single environmental factor, but very little was known on the interaction between these relationships and their combined effect on phytoplankton growth (Geider et al., 1998). In this section, we summarize the outcomes of two models taking into consideration acclimation to light, nutrients and temperature.

Cloern et al. (1995) gathered the results of some 219 experiments conducted on phytoplankton cultures exposed to either light or nutrient limitations, in steady state. Their aim was to develop an empirical function describing the variability of the Chl:C ratio that could be used to calculate phytoplankton growth rate, which cannot be routinely measured *in situ*. The authors based their function on four main observations from the literature linking the Chl:C ratio and the growth rate. Firstly, the Chl:C ratio seems to have a lower limit of about 0.003 mg.mg^{-1} (Falkowski et al., 1985). Secondly, the Chl:C ratio increases linearly with the nutrient-limited growth rate under fixed light and temperature conditions (Laws and Bannister, 1980). Thirdly, light conditions imposed to the culture influence the linear relationship between the growth rate and the ratio (Geider, 1987). Eventually, the ratio is linked to the temperature in an exponential way (Geider, 1987). Based on these observations, the following function was established (Cloern et al., 1995):

$$Chl:C = 0.003 + A\ exp(BT)\ exp(-CI)\ \mu' \tag{5}$$

where T is the temperature (°C) and I is the daily irradiance (mol.quanta.m^{-2}.day^{-1}). The factor μ' can be defined as the nutrient-limited growth rate normalized to the maximum growth rate under nonlimiting nutrient conditions and is often calculated using a Michaelis-Menten function of the most limiting nutrient. After fitting the 219 experimental observations to this equation, the parameter A was set equal to 0.0154, B to 0.050 and C to -0.059. Then, the growth rate can be calculated by inserting the ratio into this equation (Cloern et al., 1995):

$$\mu = 0.85P^B(Chl:C) - 0.015 \tag{6}$$

where P^B is the biomass-specific photosynthetic rate (mg C (mg Chl d)$^{-1}$), which depends on irradiance. This equation allows to calculate the growth rate of natural phytoplankton populations that are limited by light, nutrients and temperature simultaneously (Cloern et al., 1995).

Geider et al. (1996) developed a dynamic model to predict the impact of photoacclimation on phytoplankton growth and on the Chl:C ratio under nutrient-sufficient and balanced growth conditions. A year later, the same authors complemented their model by including acclimation to nutrients and temperature, as the growth rate and the Chl:C ratio do not depend on one resource alone (Geider et al., 1997). Eventually, in their last version, Geider

et al. (1998) modified the model to include the variability of the N:C ratio, and made it valid under unbalanced growth conditions. It is believed that the main purpose of this change in cellular chemical composition is to increase the growth rate when environmental conditions are not optimal (Shuter, 1979; Geider et al., 1998). Another function of acclimation is to protect the cell from potential damages in case of adverse environmental conditions such as high irradiance. Full description of the model equations can be found in Geider et al. (1998), here we will content ourselves with a more general overview.

Three indices are used to describe the chemical composition of the cell in terms of C, N and Chl, and three environmental variables are considered, i.e. irradiance, nutrient concentration, which in this case is nitrogen, and temperature. The cellular composition, together with these environmental factors, influence photosynthesis rates and nutrient uptake (Geider et al., 1998). Eventually, phytoplankton acclimation is governed by three characteristics (Geider et al., 1998):

- Pigment content is downregulated at high irradiance, and when nutrients or temperature limit the growth rate
- Light saturation or nutrient limitation of the growth rate results in the accumulation of energy-storage polymers that can be used once light is limited again or when there are enough nutrients
- Feedbacks exist between carbon and nitrogen metabolisms

The specificity of the model lays in the consideration of non steady state conditions of unbalanced growth (Geider et al., 1998). This means that processes such as photosynthesis and nutrient assimilation can be uncoupled. Figure 2 summarizes the main characteristics and dependencies of the C, Chl and N metabolisms in the model (Geider et al., 1998).

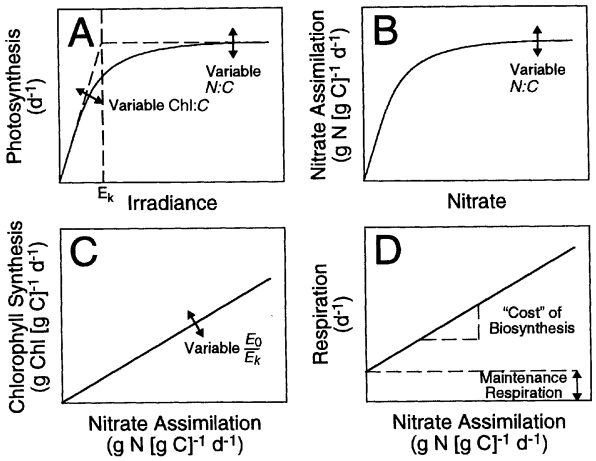

Figure 2: "[...] A. Photosynthesis is a saturating function of irradiance [...]. B. The carbon-specific nitrate assimilation is a saturating function of nitrate concentration [...]. C. The rate of Chl *a* synthesis is [...] coupled to nitate assimilation [...]. D. The carbon specific respiration rate is a linear function of the rate of nitrate assimilation [...]", from Geider et al. (1998).

The equation describing Chl synthesis in particular retains our attention and is defined as (Geider et al., 1998):

$$\frac{1}{Chl}\frac{dChl}{dt} = \frac{\rho_{Chl} V_N^C}{\theta^C} - R^{Chl} \tag{7}$$

where Chl is the concentration in chlorophyll, ρ_{Chl} is the Chl synthesis regulation term (which corresponds to the ratio of energy assimilated to energy absorbed), V_N^C is the phytoplankton carbon-specific nitrate uptake rate (this term stresses that nitrogen assimilation is necessary to complete chlorophyll synthesis), θ^C is the Chl:C ratio and R^{Chl} is the Chl degradation rate constant. The phytoplankton carbon pool varies according to this equation (Geider et al., 1998):

$$\frac{1}{C}\frac{dC}{dt} = C_{phot} - R^C - \zeta V_N^C \tag{8}$$

where C is the phytoplankton carbon, C_{phot} is the C produced through photosynthesis, R^C is the maintenance respiration rate constant and ζ is the cost of biosynthesis. It is interesting to mention that, in this model, growth depends on the internal N:C quota as this ratio is included in the calculation of the maximum photosynthetic rate. The Geider model can then be characterized as a quota model in opposition to Monod models. Quota models, also called Droop models, consider that the uptake of nutrient is regulated by internal concentrations, whereas in Monod models, nutrient uptake is dictated by external concentrations. Monod models are widely used because the environmental parameters required in the calculations are easy to measure (Sommer, 1991). However, this model can only be used under steady state conditions, so processes such as luxury uptake and storage cannot be modelled (Droop, 1983). Quota models might be more accurate in the prediction of growth rate, but they require many more prognostic variables and are associated with high computing costs (Aumont and Bopp, 2006, supporting information).

Figure 3 shows the change of the Chl:C ratio with growth rate under nutrient-limitation and for varying irradiances (Geider et al., 1998). At a given irradiance, the ratio increases with increasing growth rate. At a given growth rate, the ratio increases with decreasing irradiance.

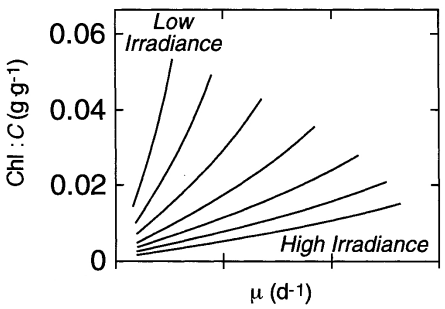

Figure 3: Dependence of the Chl:C ratio on growth rate under balanced-growth conditions, from Geider et al. (1998). Each curve describes how the growth rate and the Chl:C ratio covary with changing nutrient concentration, for a given constant irradiance.

5 Model intercomparison projects

The first initiative on ocean biogeochemical model intercomparison was launched in 1995 under the name "Ocean Carbon-cycle Model Intercomparison Project (OCMIP)". The main objective was to improve the predictive capacity of ocean carbon-cycle models by comparing and evaluating their performance in a standardized way. The first phase of OCMIP encompassed global 3-D ocean models from four modelling groups, i.e. GFDL/AOS, Hadley, IPSL and MPIM (`http://ocmip5.ipsl.jussieu.fr/OCMIP/`). Participants tried to establish protocols to make simulations and analyses as comparable as possible. This effort was maintained during the second phase of the project, with a total of 13 modelling groups this time. A good example of the outcomes of OCMIP is a paper by Steinacher et al. (2010), where four coupled carbon cycle-climate models are used to project the changes in net primary production (NPP) and export of particulate organic matter (EP) over the 21st century. They all agree on a decrease in global NPP and EP, even though the magnitude of the change varies consequently among models and regions (Steinacher et al., 2010). They also agree on the two main mechanisms responsible for the simulated changes. In low- and mid-latitudes and in the North Atlantic, NPP and EP are predicted to decrease in response to a reduced nutrient supply to surface waters due to enhanced stratification, reduced mixed-layer depth and slowed ocean circulation (Steinacher et al., 2010). In high-latitudes, an increase in NPP and EP is predicted, and the underlying mechanism is a reduction in temperature and light limitation coupled with a still sufficient nutrient supply (Steinacher et al., 2010). The only region where the models do not reach an agreement regarding the direction of the change is the Arctic. The models also differ in their predictions of Fe concentrations given that the Fe cycle is particularly difficult to model (Steinacher et al., 2010).

The "Coupled Model Intercomparison Project Phase 5 (CMIP5)" involves 20 modelling groups and also aims at reducing the differences among models and improving climate predictions. Doing so, CMIP5 provides the underlying material for future Intergovernmental Panel on Climate Change (IPCC) reports (`http://cmip-pcmdi.llnl.gov/cmip5/index.html?submenuheader=0`). Eventually, the "MARine Ecosystem Model Intercomparison Project (MAREMIP)" has the same objectives as OCMIP and CMIP5. It involves twelve modelling groups and is mainly focused on marine ecosystems, in particular the role played by different PFTs in biogeochemical cycles. A good example of the outcomes of both CMIP5 and MAREMIP is the paper by Laufkötter et al. (2015). Nine model simulations are used to project the evolution of the NPP over the 21st century under IPCC's high emission scenario (RCP8.5) (Laufkötter et al., 2015). Model predictions are not in agreement as NPP decreases in five models, increases in one and does not change significantly in three models. The region subject to more discrepancies between simulations is the belt between 30°N and 30°S. Though seven models predict a net decrease in NPP in this area, the reason behind it varies. In three models, the rea-

son for the decrease in NPP at low latitudes is an increased stratification and reduced upwelling leading to stronger nutrient limitation (Laufkötter et al., 2015). In the four remaining models, higher temperatures favour phytoplankton growth despite the stronger nutrient limitation but it also increases grazing leading to a net decrease in NPP (Laufkötter et al., 2015). One model simulates very little change in this region and the last model projects an increase in NPP due to an intensification of nutrient recycling (Laufkötter et al., 2015). Regarding the Southern Ocean, all models seem to agree on an increase in surface NPP even though the magnitude of change and the contribution of the different PFTs vary consequently (Laufkötter et al., 2015). A great number of papers focused on model comparison have been published. They can be found on the CMIP5 website (`http://cmip.llnl.gov/cmip5/publications/allpublications`) and on the MAREMIP website (`http://pft.ees.hokudai.ac.jp/maremip/index.shtml`).

Part III
Material and Methods

1 Satellite observations

1.1 Data acquisition and processing

Monthly satellite observations were downloaded from the Ocean Colour website (`http://www.oceancolour.org/`) for the period 2000-2005, for a total of 72 months. The specificity of these OC-CCI-v2.0 products lies in the fact that they are derived from the combination of data from three satellite sensors: SeaWIFs, MODIS-Aqua and MERIS. Several corrections were made to the different datasets before they were merged and the OC4v6 algorithm was subsequently applied to estimate Chl concentration at the sea surface. The detailed description of the processing goes beyond the scope of this work, but more information can be found in the online user guide (`http://www.esa-oceancolour-cci.org/`). Then, we extracted Chl concentrations from these voluminous files and the grid was converted into a 1-by-1 degree grid, using Climate Data Operators (`https://code.zmaw.de/projects/cdo`), in order to be comparable with model output. Eventually, we computed annual climatologies.

2 Model simulations

2.1 Data acquisition and processing

This study is based on 7 different marine ecosystem models. Six of them belong to the "MARine Ecosystem Model Intercomparison Project" (MAREMIP), namely REcoM2, TOPAZ, MEM, NOBM, PlankTOM5.3 and BEC. The MAREMIP data were downloaded from a Japanese server (maremip@amaterasu.ees.hokudai.ac.jp) for the period 2000-2005. The last model, i.e. PISCES, from the "Coupled Model Intercomparison Project Phase 5" (CMIP5), was run with two different Earth System Models (ESM), and will therefore be further distinguished as CNRM-PISCES and IPSL-PISCES. CMIP5 data, and more specifically the first ensemble member (r1i1p1), were found online on the Earth System Grid Federation portal (`http://esgf-node.ipsl.fr/esgf-web-fe/`) for the period 2000-2005. It is important to stress that all simulations are run with different atmosphere and ocean models. Fully coupled models (CNRM-PISCES, IPSL-PISCES, TOPAZ and BEC) allow feedbacks between ocean and atmosphere. They require a lot of computer time, which makes them quite expensive, and are therefore typically run at low resolution. Uncoupled models (REcoM2, MEM, NOBM and PlankTOM5.3) consist in an ocean model and reanalysis data as atmospheric forcing. This means that changes in the ocean will not modify the atmosphere as feedbacks are not allowed. We summarize the main characteristics of each model in Appendix A. Detailed descriptions can be found in the original

papers (REcoM2, Hauck et al. (2013); TOPAZ, Dunne et al. (2013); MEM, Shigemitsu et al. (2012); NOBM, Gregg and Casey (2007); PlankTOM5.3, Buitenhuis et al. (2013); BEC, Moore et al. (2013); PISCES, Aumont and Bopp (2006)). The reason we used those specific models lies in the number of PFTs that they take into account. Indeed, all of them consider at least 2 PFTs, diatoms and nanophytoplankton. We worked on monthly model ouputs of Chl and C and chose to focus on the surface layer. To obtain a homogeneous set of data, we converted both Chl and C values in $mg.m^{-3}$. Eventually, we computed annual climatologies.

2.2 Description of the models

Three dimensional ocean models are based on the mass balance equation describing the changes in the concentration of a tracer E with time ($\frac{\partial E}{\partial t}$):

$$\frac{\partial E}{\partial t} = \nabla(K\nabla E) - \nabla \bullet \mathbf{V}E + S(E) \tag{9}$$

where $\nabla(K\nabla E)$ is the diffusion term, $\nabla \bullet \mathbf{V}E$ is the advection term and $S(E)$ is the biogeochemical sources and sinks term. To facilitate the reading and not get lost among the many equations associated with each of the seven ecosystem models, we use two general equations describing the sources and sinks term for our tracers of interest, i.e. C and Chl. Then, we comment the relevant particularities of each model in a short paragraph, and we detail these equations in Appendix B. The complete set of equations and parameters associated with the C field are gathered by Laufkötter et al. (2015) for all models except NOBM, for which they can be found in Gregg and Casey (2007). Regarding Chl, equations and parameters are described in the reference paper of each model.

2.2.1 General equations

The sources and sinks of phytoplankton C, $S(C)$, can be described by the following equation, modified from Laufkötter et al. (2015):

$$S(C^i) = (\mu^i \times C^i) - \text{grazing} - \text{respiration} - \text{aggregation} - \text{mortality} - \text{excretion} \tag{10}$$

where i is any phytoplankton type, μ is the growth rate and C is the phytoplankton biomass. In the models, the growth rate, μ^i, can be defined as the product of the maximum growth rate μ^i_{max} and the limitations by temperature (T_f), nutrients (N^i_{lim}) and light (L^i_{lim}) as in Laufkötter et al. (2015):

$$\mu^i = \mu^i_{max} \times T_f \times N^i_{lim} \times L^i_{lim} \tag{11}$$

The only exception is NOBM, where μ is defined as follow:

$$\mu^i = \mu^i_{max} \times T_f \times min(N^i_{lim}, L^i_{lim}) \tag{12}$$

The sources and sinks of phytoplankton Chl, $S(Chl)$, can be defined as:

$$S(Chl_i) = s^i \times C^i - \text{losses} \tag{13}$$

where s^i is the Chl synthesis rate. Models vary in the number of loss terms they take into consideration, and sometimes, in the same model, the loss terms are different between the C and the Chl equations. This is expected to have an impact on the Chl:C ratio. For example, grazing does not impact phytoplankton composition, as zooplankton do not graze preferentially on C or Chl. On the other hand, Chl degradation will have an impact on the ratio as it only affects Chl.

2.2.2 Model specificities

Equations 10 and 13 are general equations and of course, discrepancies exist among models with regard to the definitions of the terms taken into consideration and the values attributed to the parameters. This probably explains part of the variability observed in model outputs and this is why we will try to briefly discuss some key particularities associated with each model.

REcoM2 is essentially based on the model developed by Geider et al. (1998), to which slight modifications have been made. Phytoplankton C is lost through excretion, respiration, aggregation and grazing, whereas Chl is lost through aggregation, grazing and degradation, meaning that the loss terms are different for the two tracers. REcoM2 is a quota model, implying that physiological rates are a function of variable intracellular ratios, i.e. N:C, Chl:C and Si:C (Hauck et al., 2013, supporting information). A fixed ratio is used to convert biomass expressed in C units to Fe concentrations (Hauck et al., 2013, supporting information). If N and Si limitations are modelled as a function of intracellular quota, Michaelis-Menten kinetics allow to model the limitation of growth caused by external Fe concentration. The growth is limited by the scarcest nutrient, following Liebig's law. An Arrhenius function is used to account for faster growth at higher temperatures and the light limitation is parameterized like in Equation 4 (Hauck et al., 2013, supporting information). As in Geider et al. (1998), Chl synthesis is proportional to N assimilation and to a regulation term representing the ratio of energy assimilated to energy absorbed (Hauck et al., 2013, supporting information).

In TOPAZ, phytoplankton growth physiology is based on the work of Geider et al. (1997) although some modifications have been made (Dunne et al., 2013). Phytoplankton C is lost through grazing. Cellular stoichiometry follows a fixed C:N ratio of 106:16 and variable Fe:C, Si:C and P:C ratios. Growth is influenced by temperature as in Equation 3, and by light as in Equation 4, except that the Chl:C ratio includes the memory of irradiance over the scale of 24 hours. Limitation by N is calculated as a Michaelis-Menten term but taking into account the preferential uptake of NH_4 over NO_3 (Dunne et al., 2013, support-

ing information). Si limitation is also represented by a Michaelis-Menten term. Growth is further limited by the amount of P and Fe in the cell by a quota-type approach, then Liebig's law is applied (Dunne et al., 2013, supporting information). Chl is a diagnostic variable calculated from the C:N ratio and intracellular N concentration.

In PISCES, phytoplankton C and Chl are lost through exudation, mortality, aggregation and grazing, so the loss terms are the same for both tracers. PISCES can be considered as a Monod model given that the relative concentration of C, N and P is regulated by a Redfield ratio of 122/16/1 and that phytoplankton growth is influenced by the external concentrations of N, P, Fe and Si following Michaelis-Menten kinetics (Aumont and Bopp, 2006, supporting information). But it can also be defined as a quota model given that the elemental ratios of Fe, Chl and Si are not constant (Aumont and Bopp, 2006, supporting information). To determine which nutrient limits the growth most, Liebig's law is applied. Light limitation is modelled as in Equation 4 and the temperature dependence is based on Equation 3 (Aumont and Bopp, 2006, supporting information). Chl synthesis is proportional to the growth rate and to the ratio of energy assimilated to energy absorbed which is defined in Geider et al. (1996).

In MEM, phytoplankton C is lost through respiration, excretion, mortality and grazing. Cellular stoichiometry follows a fixed C:N ratio of 106:16 and Fe and Si concentrations are optimized according to N concentration. The uptake of N, Fe and Si is modelled using the optimal uptake kinetics proposed by Smith et al. (2009) and Liebig's law is subsequently applied to determine the most limiting nutrient. Growth is dependent on temperature following Equation 3 and on light following the formula developed by Platt et al. (1980). Chl concentration is calculated from phytoplankton biomass using a constant C:Chl ratio of 125 and 50 µg μg^{-1} for small phytoplankton and for large phytoplankton respectively (Shigemitsu et al., 2012).

In NOBM, phytoplankton C is lost through aggregation, exudation, respiration, grazing and mortality. Cellular stoichiometry is based on the Redfield ratio. Michaelis-Menten functions are used to describe the dependence of the growth rate on nutrients, i.e. N, Fe and Si, but also on total irradiance (Gregg and Casey, 2007). The most limiting factor is determined by the Liebig's law. The relationship between growth and temperature is based on Eppley (1972). The Chl field is calculated from the C:Chl ratio, which is not constant (Gregg and Casey, 2007). The authors use three different light states, a low, a medium and a high one, to which they attribute a different ratio in order to account for photoadaptation. Then, the ratios are linearly interpolated for irradiances falling between the three reference light levels (Gregg and Casey, 2007).

In PlankTOM5.3, the internal composition varies with regard to Fe:C, Si:C and Chl:C ratios, and follows fixed ratios regarding the macronutrients. Phytoplankton C and Chl

are lost through the same processes, i.e. exudation, grazing and general loss term encompassing respiration, aggregation and mortality (Buitenhuis et al., 2013). The growth rate is dependent on N and Si external concentrations (Michaelis-Menten approach) and on Fe internal composition (quota approach) (Buitenhuis et al., 2013). Liebig's law is then applied to determine the scarcest nutrient. The dependence of the growth rate on light is described by Equation 4 and the temperature dependence is based on Eppley (1972). Chl synthesis rate is proportional to the growth rate and to a regulation term which is the ratio of energy assimilated to energy absorbed (Buitenhuis et al., 2013).

In BEC, phytoplankton C and Chl are lost through the same processes, i.e. grazing mortality, non-grazing mortality and aggregation. Phytoplankton internal composition varies with respect to Chl:C, Fe:C and Si:C ratios but has a fixed C:N:P ratio of 117/16/1 (Moore et al., 2013). The growth rate depends on external concentrations in Fe, N, Si and P following a Michaelis-Menten approach. Again, Liebig's law is applied. Light limitation is described by Equation 4 and the relationship between temperature and growth is based on Eppley (1972). As in PlankTOM5.3, Chl synthesis rate is proportional to the growth rate and to a regulation term which is the ratio of energy assimilated to energy absorbed.

Part IV
Results and discussion

1 Comparison of chlorophyll simulations with observations

Models have been evaluated individually in their descriptive papers, therefore we will only focus here on one variable of interest, i.e. Chl. The aim of this section is to assess the ability of the eight model simulations to represent the Chl field. For that purpose, we will consider satellite observations as reference values, compare them with model outputs and evaluate their degree of agreement. This will be achieved in three steps: firstly, by comparing global maps visually, secondly, by looking at the distribution of Chl averaged over latitude for both satellite and models, thirdly, by summarizing the statistics of (dis)agreement by a so-called Taylor diagram. Eventually, we will try to explain where the discrepancies between satellite observations and model simulations may arise from.

1.1 Global maps

In this subsection, global maps are presented of the annual climatology of total Chl in surface waters, averaged over six years, from 2000 until 2005, for satellite data (Figure 4), and for model simulations (Figure 5). Maximum Chl concentrations go up to 47.8 mg m^{-3}, 3.9 mg m^{-3}, 2.0 mg m^{-3} and 3.0 mg m^{-3} for satellite observations, CNRM-PISCES, IPSL-PISCES and BEC, respectively. The five remaining simulations have maximum values lower than 1.5 mg m^{-3}. Therefore, for the purpose of this visual comparison, we chose to set arbitrarily the maximum value of the color scale to a Chl concentration of 1.5 mg m^{-3}. This should increase the contrast and make patterns more apparent. Satellite observations show that high concentrations in Chl are essentially found in coastal regions, whereas open ocean values rarely exceed 1.0 mg m^{-3}. Gyres, in particular, can be easily localised due to their very low Chl concentrations, close to 0 mg m^{-3}. By comparing Figure 5 with Figure 4, it is clear that models do not simulate the very high coastal concentrations observed in satellite data due to their coarse resolution, with the exception maybe of CNRM-PISCES, IPSL-PISCES and BEC. Indeed, these three models present values slightly higher than 1.5 mg m^{-3} in some coastal regions of the world but still not as high as the observations. Regarding Chl concentrations in the open ocean, models seem to simulate them pretty well, with values ranging from around 0 in gyres and up to around 1 mg m^{-3} in productive regions, which is quite satisfying. If we now compare the results of the eight model simulations, we notice some differences. They generally agree on the fact that gyres are low Chl areas, but their extent varies greatly. For example, they are barely distinguishable in BEC, and they cover almost all the area between 40°N and 40°S in CNRM-PISCES and IPSL-PISCES. Another striking difference can be observed in the Equatorial Pacific. All models simulate a tongue of higher Chl concentration starting at the western boundary of the American continent. However the length and the width of this

tongue, as well as its concentration of Chl differ among models. In MEM, the Equatorial Pacific is the area with the highest concentrations in Chl and in PlankTOM5.3, CNRM-PISCES and IPSL-PISCES, the same area can barely be distinguished. Some models simulate very localised peaks of Chl such as BEC in the Southern Ocean and the Bering Strait, whereas others seem to represent a rather homogeneous Chl pattern throughout the world oceans, i.e. NOBM and PlankTOM5.3. Eventually, maximum Chl values can differ from almost one order of magnitude among models, as in CNRM-PISCES (3.9 mg m^{-3}) and NOBM (0.5 mg m^{-3}). However, despite these rather quantitative differences among models that we will try to explain later in this work, we can reasonably say that the patterns in Chl distribution are comparable with the observations, at least for the open ocean.

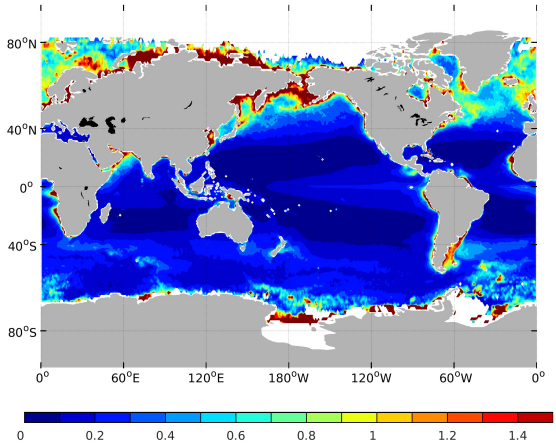

Figure 4: Annual climatology of total Chl in surface waters (mg m^{-3}) from satellite observations

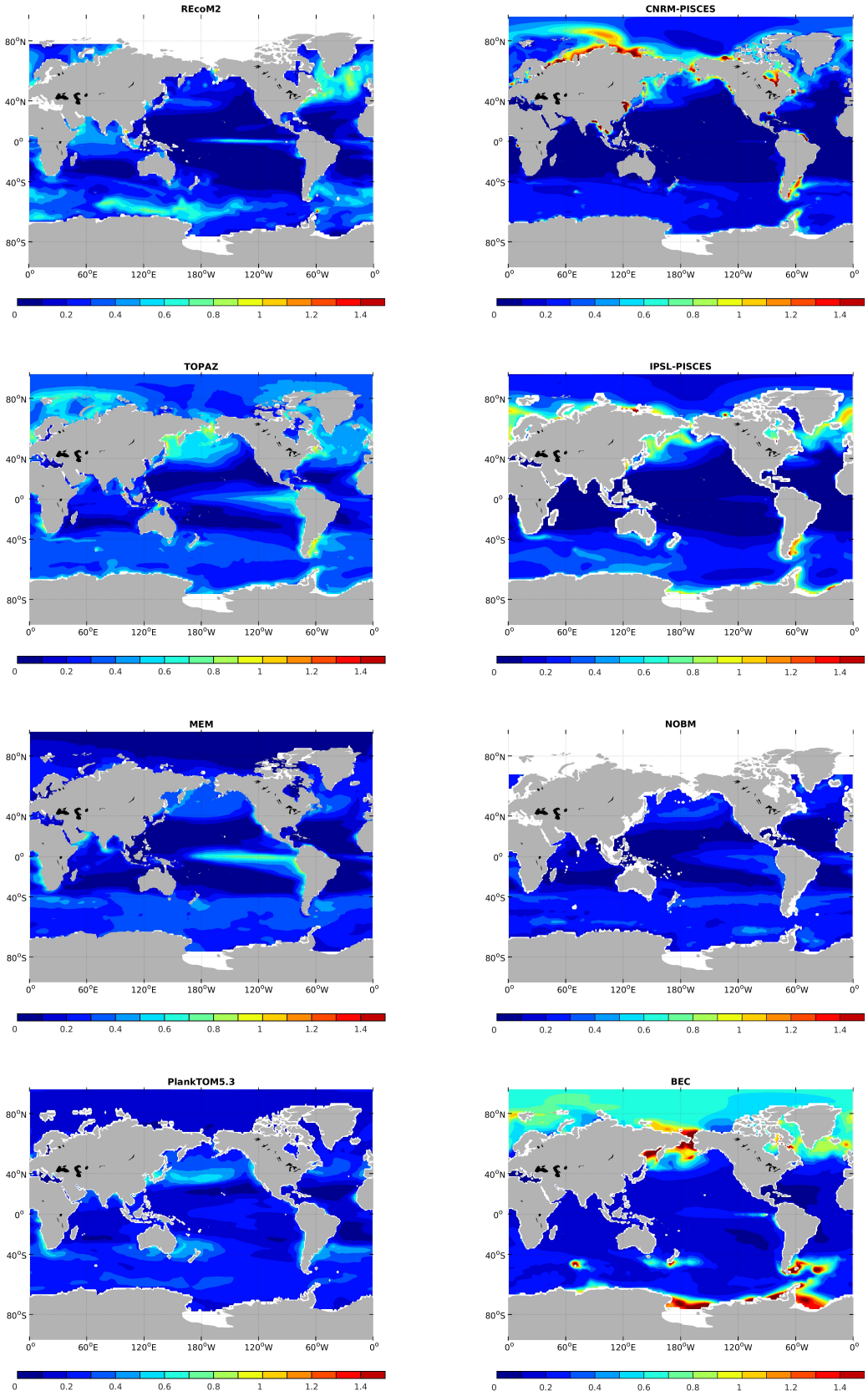

Figure 5: Annual climatology of total Chl in surface waters (mg m^{-3}) from model simulations

1.2 Chlorophyll versus latitude

A slightly more quantitative way to assess the simulated Chl field is to plot the annual climatology of averaged Chl as a function of latitude for each model. Then, we compare the latitudinal distribution to the one generated for satellite observations. Figure 6a shows that models are globally in agreement regarding the distribution of the Chl field with latitude. The general pattern is a peak in Chl between 40 and 60°S, a minimum around 20°S, then a peak around the Equator, a minimum around 20°N, and eventually an increase between 40 and 60°N. If the trend is comparable, some differences can still be highlighted. Indeed, peaks and troughs do not occur at the exact same latitude and have different widths and amplitudes. This is particularly apparent in high northern latitudes, where models seem to diverge more than elsewhere. This is also apparent in the BEC model, where the mean Chl peaks up to 1.5 mg m^{-3} around 80°S and to more than 1 mg m^{-3} around 60°N whereas the mean Chl in the seven other models is mostly comprised between 0 and 0.5 mg m^{-3}. CNRM-PISCES and IPSL-PISCES have notably lower values of Chl around the Equator compared with the six other models. We can also notice that TOPAZ, BEC, CNRM-PISCES and IPSL-PISCES peak around 80°S, a behaviour that is not seen in other models. The same pattern is observed in satellite data, Figure 6b, with mean Chl concentrations reaching 2.5 mg m^{-3} at that latitude. This could be explained by the extremely productive Ross Sea, where Chl concentrations as high as 14.6 mg m^{-3} and mean concentrations of 2.5 mg m^{-3} were measured in situ (Arrigo et al., 2008a). Another Chl peak can be observed around 60-70°N in satellite data. According to Pabi et al. (2008), the mean Chl concentration in the Arctic can reach 2.5 mg m^{-3} during the spring bloom in April-May, and the summer bloom during July-August and remain quite high in between, i.e. 1.5 mg m^{-3}, which is in agreement with the concentrations seen in Figure 6b. An unexpected peak of Chl occurs around 80°N. It could be explained by a recession of the sea ice, allowing the development of phytoplankton in areas previously not free of ice. To verify this hypothesis we decreased the number of years taken into consideration and realised that from 2000 until 2001, there is no Chl peak around 80°N. The peak appears in the following years. We searched in the literature for confirmation and found a study from Arrigo et al. (2008b) mentioning that the shrinking of sea ice cover has accelerated in the Arctic since 2002, which is totally in agreement with our model results. Sea ice extent was particularly low in 2005. Areas more affected by sea ice losses were the Siberian, Laptev and Chukchi sectors of the Arctic Ocean (Arrigo et al., 2008b). The extension of open water areas helped to boost primary production, particularly in these three sectors. In summary, except for the higher amplitude in high latitude regions for satellite data, the latitudinal distribution obtained from simulations are still reasonably comparable with the satellite data.

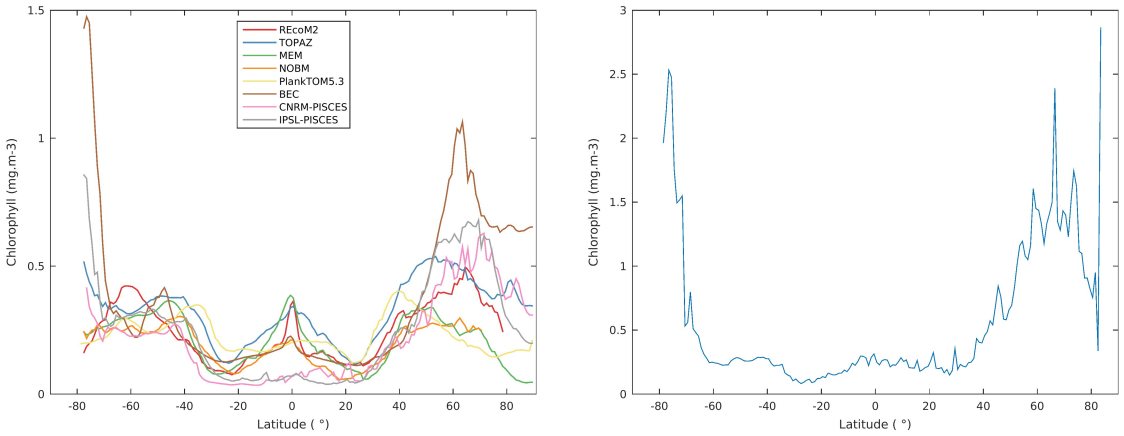

(a) Model simulations

(b) Satellite observations

Figure 6: Annual climatology of averaged Chl as a function of latitude. Note the different scale for the two plots.

1.3 Taylor diagrams

We used a Taylor diagram to assess, in a statistical way, the degree of agreement between satellite observations and model simulations regarding the patterns of the annual climatology of the Chl field (Taylor, 2001). The correlation, the standard deviation and the root-mean-square error (RMSE) between patterns are summarized in a single diagram which is presented in Figure 7. Each model corresponds to one point on the diagram. It is important to stress that we used the logarithm of Chl concentrations here. Indeed, as Chl concentrations are not normally distributed, it makes more sense to calculate their logarithm prior to statistical analysis. The correlation between the observed field (letter A) and the simulated field for each model (letters B to I) is given by the azimuthal position of a point in the diagram, delimited by blue dash-dotted lines. PlankTOM5.3 has the lowest correlation with satellite data, i.e. 0.56, and TOPAZ, the highest, i.e. 0.71. The standard deviation of a pattern is represented by the radial distance from the origin (black dotted lines). Two distinct groups seem to appear. The first one, composed by REcoM2, CNRM-PISCES, IPSL-PISCES and MEM, slightly overestimates the standard deviation seen in satellite data, which means that the average deviation from the mean Chl is higher in those models than in the satellite observations. The second group underestimates it, slightly for TOPAZ and NOBM, more considerably for BEC and PlankTOM5.3. Eventually, the RMSE between the observed and simulated fields is represented by the green dashed lines, and is approximately equal to 0.3 in logarithmic units for all models. In summary, models reasonably simulate the Chl field, even though progress is still required to get closer to observations. No model seems to give much better results than the others, however, we can identify PlankTOM5.3 as the poorest performer in representing the annual mean patterns of Chl. The same exercise was done for monthly climatologies of four representative months, namely January, March, July and September, and the corre-

sponding Taylor plots are shown in Appendix C. Correlations are generally lower, standard deviations higher, and the two groups identified for the annual climatology no longer exist. Some models still give reasonable results, particularly TOPAZ and NOBM. Others are much less convincing such as REcoM2 and MEM. This leads us to conclude that models are less accurate in predicting the correct timing of the seasonal cycle than the annual mean.

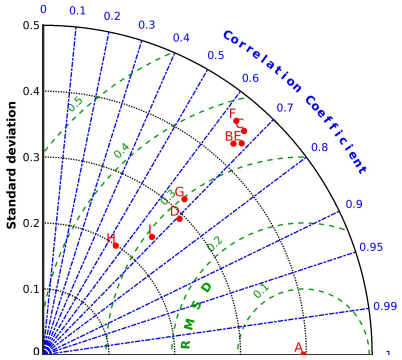

Figure 7: Taylor diagram showing the correspondence between model simulations and satellite observations with regard to the annual climatology of Chl in surface waters. A=Observations, B=REcoM2, C=CNRM-PISCES, D=TOPAZ, E=IPSL-PISCES, F=MEM, G=NOBM, H=PlankTOM5.3, I=BEC.

1.4 Discrepancies between satellite observations and model simulations

In the light of this first three-steps analysis, we can conclude that, even if they capture general patterns, models do differ from satellite observations in the way they simulate the Chl field. We will therefore try to develop some of the reasons explaining the discrepancies between satellite observations and model simulations.

Firstly, by computing the Chl annual climatology from satellite observations, we generate a bias towards summer in high latitude regions. Indeed, satellite observations are sparse during winter months in these areas as there is barely any light, which prevents Chl measurements. The annual mean is therefore based almost exclusively on summer Chl values, which is likely to increase the average and explain the high Chl concentrations in high latitudes regions in Figure 4.

Another explanation is that satellites are able to capture very high coastal Chl values, arising from processes that most models are not yet developed enough to represent. There are three main reasons for that:

- The first reason is that, in order to avoid a too small time step, models need a coarse resolution to be numerically stable. Indeed, finer grids can be numerically stable but with a much smaller time step, which requires enormous computational resources, outside our reach. The eight model simulations we consider have a 1 by 1 degree grid, or have been interpolated to that grid for our analyses, which is too coarse

too represent the small scale processes occurring in coastal areas. Moreover, most models require at least three grid points in the vertical direction, that is why they cannot resolve shallow environments properly. Indeed, as depth is averaged over the extent of this 1 by 1 degree box, deep areas weigh more in the balance and shallow shelves disappear in the mean. However, these shallow waters receive a lot of light and are the site of what is called bentho-pelagic coupling. This coupling favours primary production by ensuring a rapid turnover of nutrients (Marcus and Boero, 1998). These coastal areas rich in Chl are therefore not well represented in most models.

- The second reason is that most models do not consider the riverine input, which is a major source of nutrients in coastal regions, stimulating primary production and therefore increasing Chl concentrations. PISCES is the exception as it provides an annual mean river discharge of dissolved organic and inorganic carbon with a supply of nutrients derived from constant Fe/P/N/Si/C ratios (Aumont and Bopp (2006), supporting information). Higher Chl values can be seen in figure 5, for CNRM-PISCES and IPSL-PISCES, at the estuary of the Amazon river for example.

- A third explanation is that coastal upwelling is typically too weak in model simulations. This is at least partially due to the atmospheric forcing which is represented on a coarse grid of about 2 by 2 degrees. Therefore, it prevents resolving small scale winds that play an important role in the upwelling process.

To assess the impact of these structural differences, we reproduced the graphs made in subsection 1.2, but this time we applied two corrections. To account for this bias towards summer in satellite data, we chose to consider only model data for which we have a satellite equivalent. And to account for the fact that models fail in the representation of high Chl concentrations in coastal regions, we set an arbitrary threshold of 5 mg m^{-3}, and only considered Chl values lower than this threshold. This is of course only to assess qualitatively how high coastal values and the summer bias affect the annual climatology, and maybe get a closer match between satellite and model data. The results are presented in Appendix D. We can see on the graphs that the modelled Chl distribution is now more similar to the observed one. The BEC model even seems to follow quite well the satellite profile.

2 Chlorophyll to carbon ratio

The computation of primary production is essential if we want to fully understand the importance of phytoplankton in the C cycle. According to Sathyendranath et al. (2009), ecosystem models used for this purpose require four basic parameters, namely the initial slope of the photosynthesis-irradiance curve, the light-saturation parameter of that curve, the specific absorption coefficient of phytoplankton and the C:Chl ratio of phytoplankton. While the first three parameters can be easily measured, the C:Chl ratio is still subject to great uncertainty as the relationship between phytoplankton C and Chl is not strictly linear (Sathyendranath et al., 2009; Geider et al., 1998). It is therefore crucial to increase our knowledge on this parameter in order to refine ecosystem models. This is why this section is dedicated to the annual climatology of the Chl:C ratio in model simulations. The use of a Chl:C or C:Chl ratio is arguable, although equivalent. We choose to work on the first one to avoid infinite ratios as Chl can reach very low concentrations in some models. Our main objective is to understand the sources of discrepancies between models. To achieve this goal, we carry out three types of analyses. We use global maps to obtain a first general overview of the Chl:C ratio distribution in surface waters. As the ratio is both nutrient- and light-dependent, and as these are not equally distributed with latitude, we then analyze the meridional dependence of the ratio. Eventually, we plot the annual climatological values of C versus Chl in surface waters in order to understand better how these two variables behave towards each other and how models deal with this relationship. In these three subsections, we describe the results and hypothesize the potential sources of the differences or similarities in the ratio among models, then try to confirm or reject these hypotheses by having a closer look at the equations behind the Chl:C ratio.

There are two ways of calculating the annual climatology of the Chl:C ratio. The first one is to calculate the ratio for each month at every grid point and then average this ratio over the 72 months taken into consideration (mean of the ratios). The second way is to average the C and the Chl individually over the 72 months, and then calculate the ratio for every grid point (ratio of the means). Both methods are correct, however the second one may have more biogeochemical relevance. Indeed, it is equivalent to calculating the average ratio weighted by the total biomass:

$$\frac{\sum_{i=1}^{72} Chl_i}{\sum_{i=1}^{72} C_i} = \frac{\overline{Chl}}{\overline{C}} = \frac{1}{72}\sum_{i=1}^{72} \frac{Chl_i}{C_i} \cdot \frac{C_i}{\overline{C}} \tag{14}$$

where i is the number of months considered, 72 in this study. This means that months with high biomass will influence the ratio more than months with low biomass. Therefore, we choose to use this method to calculate the annual climatology of the Chl:C ratio. However, it is important to mention that, due to the relationship to light, there is a strong seasonality

in the Chl:C ratio, especially in high latitudes, and therefore, the results obtained with this method might be somewhat different from the ones that would be obtained with the first method.

2.1 Global distribution

The main advantage of global maps is that they provide a rapid and rather qualitative overview of the distribution of a variable. Figure 8 shows the simulated annual climatology of the Chl:C ratio in surface waters. The maximum value of the ratio is 0.045, 0.038 and 0.037 mg mg^{-1} in TOPAZ, REcoM2, and CNRM-PISCES, respectively. The five other model simulations have maximum ratios lower than 0.03 mg mg^{-1}. This range of values is in agreement with the laboratory data compilation by Behrenfeld et al. (2002), where the Chl:C ratio was comprised between 0.001 and more than 0.06 mg mg^{-1}. Dunne et al. (2005) gathered field observations from some 40 oceanographic studies and obtained a Chl:C ratio ranging between 0.007 and 0.05 mg mg^{-1}, which is also comparable with the results generated by simulations. The only model that has minimum values lower than 0.001 is REcoM2 with $4.2 \cdot 10^{-7}$ mg mg^{-1}.

The first striking observation is that all the models, except REcoM2 and NOBM, present a low ratio within the 40°S-40°N belt, with even lower values in gyres, a tongue of somewhat elevated Chl:C ratio around the Equatorial Pacific and a high ratio at higher latitudes. This statement seems to be in agreement with the theory of the Geider model which states that the ratio decreases with nutrient limitation, typically in the gyres, and increases with light limitation, typically in polar regions. However, as we are studying the annual climatology of the ratio, the impact of light limitation, in particular, might be attenuated in the mean. To account for that, we look at two typical winter and summer months, namely January and July. The maps are presented in Appendices E and F. It clearly appears that the six models we mentioned above present a strong seasonality. In January, the ratios are comparatively higher in the Arctic. This might arise from the ice cover. Indeed, ice reduces the amount of light reaching the sea surface, and this phenomenon is therefore represented as light limitation leading to an increased Chl:C ratio. In July, the pattern is a bit less contrasted than in January, as some of the six models present a higher ratio in both polar regions, particularly CNRM-PISCES and IPSL-PISCES. Antarctic sea ice extent reaches a maximum in winter, which is modelled as a strong light limitation and therefore a high ratio. In the Arctic, the ice cover is still present in July, though smaller than in January, which explains why the ratios are still quite high in this region even though it is summer.

The second thing to notice is that, except for the low Chl:C ratio in the gyres and the comparatively higher ratio in equatorial waters, REcoM2 behaves quite differently from the six models described above. The Southern Ocean (as this set-up of REcoM2 does not model regions north of 80°) shows a very low Chl:C ratio, whereas much higher ratios are

seen in the Indian Ocean, the Equatorial Pacific and the west coast of Africa. So there have to be other processes involved that can explain this distribution. A hypothesis could be that Fe limitation in the Southern Ocean is stronger in REcoM2 than in the other models for example. Other parameters that could be studied to explain why REcoM2 behaves so differently regarding the Chl:C ratio are the Chl degradation rate and the type of growth considered by the model, i.e. balanced or unbalanced. This will be further developed in section 3.

Eventually, it is interesting to highlight that NOBM has a constant ratio of 0.0064 everywhere. By having a closer look at the reference paper, we notice that NOBM considers that the ratio is only influenced by light (Appendix B5). Gregg and Casey (2007) use three different light states, a low, a medium and a high one, to which they attribute a different ratio based on laboratory experiments, in order to account for photoadaptation. Then, the ratios are linearly interpolated for irradiances falling between the three reference light levels. As the ratio is constant, it probably means that the average annual light level at the sea surface is everywhere higher than the high light state defined in Gregg and Casey (2007), and therefore set equal to this high light state value.

It is important to not only rely on maps but also to proceed to an analysis of the structural equations behind the models. Indeed, based on Figure 8, one could think that the Chl:C ratio in MEM varies with environmental conditions, but the dependency on those conditions is actually only indirect. MEM actually uses a fixed ratio to convert C into Chl (Appendix B4). The reason why the global map does not show a uniform pattern is because the Chl:C ratio for diatoms is higher than for nanophytoplankton, which is in agreement with the findings of Sathyendranath et al. (2009). As the relative abundance of these two PFTs in the total phytoplankton biomass varies, the distribution of the ratio varies as well.

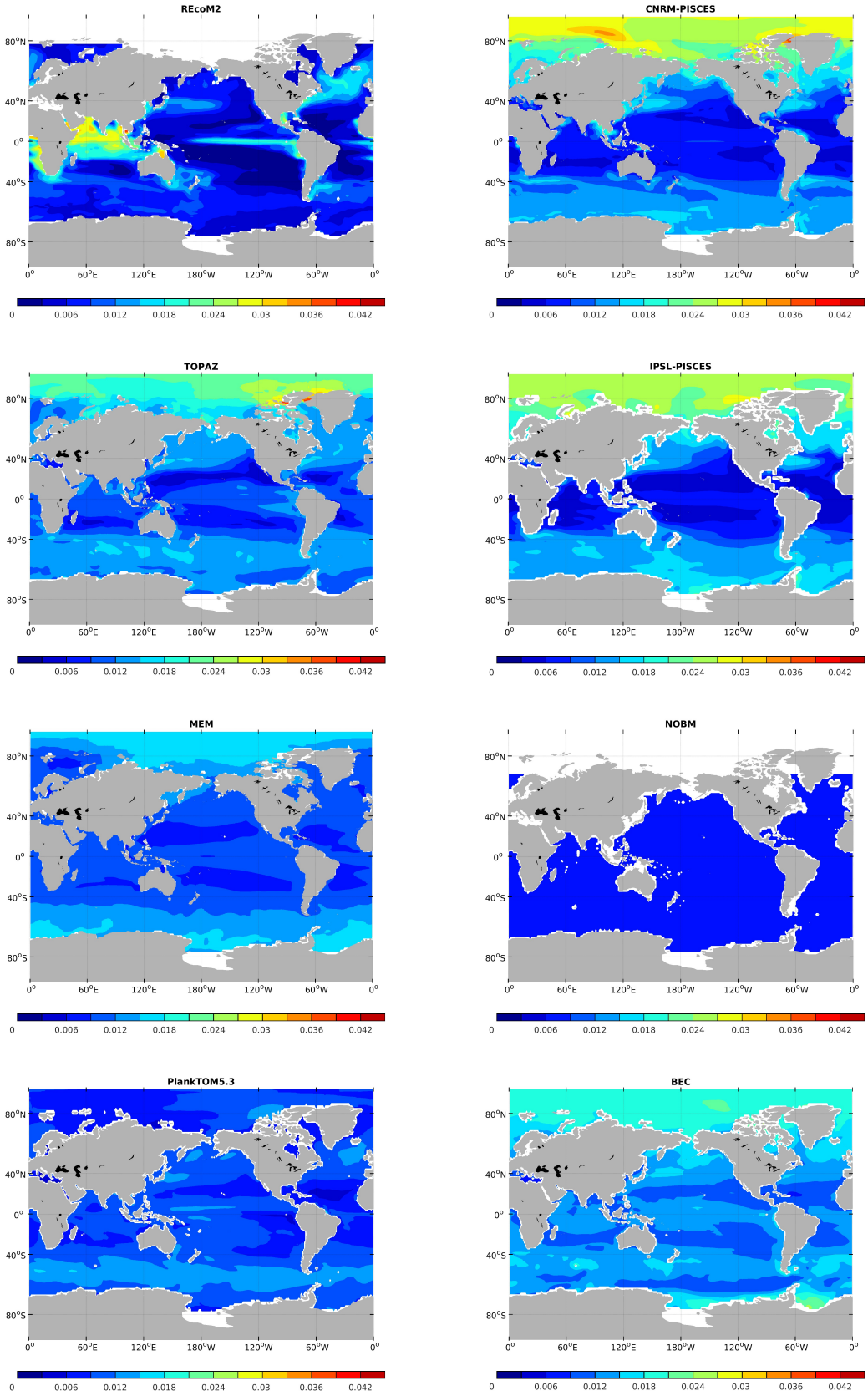

Figure 8: Annual climatology of the Chl:C ratio (mg mg^{-1}) in surface waters from model simulations

2.2 Meridional distribution

In this subsection, we study the meridional distribution of the surface Chl:C ratio in the eight model simulations, represented by solid lines in Figure 9. All models, except REcoM2 and NOBM, seem to agree on the trend of the meridional dependence of the ratio. It is high in polar regions, with higher values in the Arctic than in the Southern Ocean, then decreases to reach a minimum in the gyres, then increases slightly around the Equator. CNRM-PISCES and IPSL-PISCES show relatively lower values within the 20°S-20°N belt and higher values in the Arctic. TOPAZ has accentuated troughs in the gyres and the curve in BEC is particularly flat. As previously mentioned, NOBM has a constant ratio over the world oceans. The behaviour of the ratio in REcoM2 is very different. The ratio presents very low values of about 0.005 mg mg^{-1} around 80° both in the Northern and Southern hemispheres, and increases progressively to reach about 0.01 mg mg^{-1} around 40°S and N. Then it decreases in the gyre areas, and peaks up to 0.015 mg mg^{-1} at the Equator. The trend might be comparable with the other models between 40°S-40°N even though the amplitude is much higher in REcoM2. But in polar regions, the trend is completely opposite. An important point to make here, is that we did not represent the variability associated with seasons or longitude for each model on this graph. It would indeed make more sense to show some measure of variability such as the standard deviation for example. Unfortunately, this would greatly alter the readability of the graph so we chose to leave it as it is. Field observations of Chl:C ratio compiled by Dunne et al. (2005) are plotted in function of latitude as well in order to allow comparison between simulations and *in situ* data. The spatial coverage is limited, there is no data between 20 and 50°S for example, and the temporal coverage is only punctual, so it gives only a rough idea of the ratio at some latitudes. It is important to stress that these data have not been zonally averaged which could be the reason why model simulations and field observations do not seem to concur. This makes us realize that there is a crucial need to extent the spatial and temporal coverage of *in situ* measurements of the Chl:C ratio in open oceans in order to enhance the accuracy of model calibration and therefore lead to less uncertain predictions.

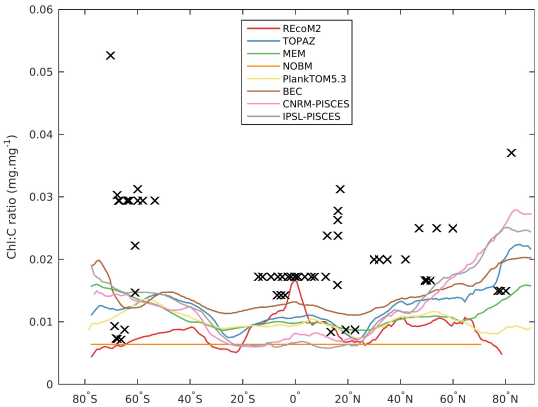

Figure 9: Annual climatology of averaged Chl:C ratio (mg mg^{-1}) as a function of latitude in surface waters from model simulations (lines) and from the data compilation by Dunne et al. (2005) (black crosses).

More recently, Graff et al. (2015) published phytoplankton C concentrations directly measured in the open ocean during two cruises. Such measurements are extremely rare and precious given the difficulty to isolate the fraction of particulate organic C actually associated with phytoplankton. They also developed an approach to assess C biomass based on particulate backscattering coefficients (b_{bp}), which is a property that can be retrieved from satellite observations (Graff et al., 2015). The method seems quite promising given the high correlation between the proxy and direct measurements. The authors also measured Chl concentrations in their samples and reported the C:Chl ratios from the Atlantic cruise on a graph. The ratios were comprised between 31 and 358 µg $µg^{-1}$, which is equivalent to a Chl:C ratio between 0.0027 and 0.032 µg $µg^{-1}$. They complemented their measured values with estimations optically derived from b_{bp}. This graph is presented in Appendix G. We also added a revised version of Figure 9 in Appendix G, but presenting the C:Chl ratio between 50°N and 50°S in order to facilitate comparison with the plot from (Graff et al., 2015). In the northern gyre, REcoM2 overestimates the C:Chl ratio whereas the other models are quite close to observations. But in the southern gyre, REcoM2 seems to represent the C:Chl ratio quite well, whereas the other models underestimate it. Globally, with the exception of NOBM, models and observations present a similar trend, which is quite encouraging for modellers.

2.3 Carbon versus chlorophyll

This analysis will allow us to investigate the relationship between C and Chl in each of the eight model simulations. The graphs are presented in Appendix H. In order to confront comparable data, Chl values lower than 10^{-2} mg m^{-3} were discarded from this analysis as some models do not simulate very low Chl concentrations. The linear regression of the log-transformed data and its equation are superimposed on each graph. The slopes vary from 0.44 in REcoM2 to 1 in NOBM as this model considers a strictly linear relationship between C and Chl. So except for NOBM, all the models agree on a slope lower than 1. This means that for a certain increase in C, the increase in Chl will be larger. We can also notice that REcoM2 shows the largest range of C concentrations associated with one Chl value. So, according to REcoM2, biomass estimations from Chl measurements can vary by one order of magnitude. The regression line equations can be compared with the work of Sathyendranath et al. (2009) where the relationship between particulate organic carbon (POC) and Chl is used to estimate phytoplankton C. They assume that, in POC measurements, for any Chl concentration, the minimum associated POC concentration corresponds to phytoplankton (Sathyendranath et al., 2009). Then, quantile regression (q=0.01) is used to fit a line linking the minimum values. As they measured Chl concentrations with two different methods, they obtained two different equations describing the relationship between phytoplankton C and Chl, both in mg m^{-3}:

$$C = 79 \times (Chl)^{0.65} \tag{15}$$

$$C = 64 \times (Chl)^{0.63} \tag{16}$$

These two lines were superimposed on the graphs in Appendix H for comparison. Their slopes, both lower than 1 as well, are steeper than the slope of the regression lines of REcoM2, CNRM-PISCES, IPSL-PISCES and TOPAZ, but flatter than the ones of MEM, NOBM, PlankTOM5.3 and BEC. With a slope of 0.61, CNRM-PISCES is the closest from the results obtained by Sathyendranath et al. (2009) in Equations 15 and 16. We can therefore conclude that there is an agreement among models and with the work from Sathyendranath et al. (2009) that the linear regression between the log-transformed C and Chl has a slope lower than 1.

3 Focus on REcoM2

In the previous section, we highlighted that models have different ways of dealing with the Chl:C ratio. It appears that the eight model simulations can be divided into a "constant ratio" category, comprising MEM, a "light-dependent ratio" category, comprising NOBM, and a "variable ratio" category, comprising the six remaining simulations. In this latter category, all the models acknowledge the influence of temperature, light and nutrients on the ratio, however, we saw in subsection 2.2 that the latitudinal pattern of the Chl:C ratio in REcoM2 is significantly different from the others. To understand better the reasons behind this divergence, it is necessary to proceed to some further analyses. In this section, we decided to make a distinction between the two PFTs taken into consideration by REcoM2, i.e. diatoms and nanophytoplankton, as it helps to understand the mechanisms of change when looking at them separately. We will first have a look at maps presenting the distribution of the dominant limiting nutrient for both PFTs in all the simulations. Then, we will discuss the very low minimum values of the Chl:C ratio in REcoM2. The third analysis will focus on the dependency of the Chl:C ratio on growth rate under light and nutrient limitation in REcoM2. In the fourth subsection, we will discuss the hypothesis that REcoM2 is able to predict the behavior of the ratio under non steady state conditions as in Geider et al. (1998). Eventually, we will proceed to a sensitivity analysis on two parameters, i.e. the Chl degradation rate and the maximum Chl:N ratio.

3.1 Nutrient limitations

The first question we would like to answer is why does REcoM2 have very low Chl:C ratios in the Southern Ocean compared to other simulations? A likely hypothesis would be that some nutrient limitation in this region is stronger in REcoM2 than in the other models. We had to discard two models from this analysis given that the ratio in NOBM is only influenced by light and that we do not have the required information to calculate nutrient limitations in TOPAZ. In the models, the limitation can be expressed by a number between 0 (full limitation) and 1 (no limitation) for each nutrient. One can therefore analyze which of the limitation factors is lowest. The distribution of the dominant limiting nutrient for diatoms in the six remaining model simulations is presented in Appendix H. Fe is the most limiting nutrient for diatoms in the Southern Ocean in all models except PlankTOM5.3. After looking at the values, it appears that Fe limitation in REcoM2 is pretty much comparable with CNRM-PISCES and IPSL-PISCES, and is less strong than in MEM in the Southern Ocean. Only BEC presents a lower Fe limitation than REcoM2 in this area. This means that Fe limitation does not explain the big differences that are seen in the Southern Ocean ratio between REcoM2 and the other five models. The same graphs but this time for nanophytoplankton can be found in Appendix J. Part of the Southern Ocean is colored in dark blue in REcoM2, CNRM-PISCES, IPSL-PISCES and BEC, which means that no nutrient limitation is lower than 0.7 in the annual mean. So either there is no limitation, or light is limiting. So we can refute the hypothesis that

nutrient limitation explains why the ratio in the Southern Ocean is so different in REcoM2.

Another point we would like to make here is that, initially, Fe is not included in the Geider model. But it has been built into the Geider model in REcoM2 so that, as for the other nutrients, Fe limitation would lead to a reduction of the Chl:C ratio. However, it is not clear yet whether Fe limitation actually results in a decrease of the ratio. Indeed, some studies demonstrate that mechanisms of adaptation to Fe limitation exist (Behrenfeld and Milligan, 2013; Strzepek and Harrison, 2004). Strzepek and Harrison (2004) showed that in Fe-limited waters, oceanic diatoms can modify their photosynthetic architecture and reduce their concentrations in photosystem I and cytochrome b6f complex to lower their Fe requirements without changing their photosynthetic rates. In their review, Behrenfeld and Milligan (2013) stated that phytoplankton response to Fe limitation can include an overexpression of photosynthetic pigments relative to growth rate when macronutrient levels are high, which would therefore results in a higher Chl:C ratio. Nevertheless, what happens under Fe and light limitations together, typically in the Southern Ocean, is still a matter of active research and the parameterization of the impact of Fe stress on the Chl:C ratio needs to be further investigated.

3.2 Minimum values of the Chl:C ratio

We noticed in subsection 2.1 that REcoM2 is the only model to allow such small values for the Chl:C ratio. Indeed, while the minimum values encountered in other model simulations for the annual climatology of the Chl:C ratio are above 0.003 mg mg^{-1}, the minimum value found in REcoM2 is of the order of 10^{-7} mg mg^{-1}. This is also much lower than the minimum values reported in the literature. Behrenfeld et al. (2002) obtained values ranging from 0.001 to more than 0.06 mg mg^{-1} for laboratory experiments. In their compilation, Dunne et al. (2005) gathered ratios ranging between 0.007 and 0.05 mg mg^{-1}. Eventually, the ratios measured on the field by Graff et al. (2015) were comprised between 0.0027 and 0.032 µg $µg^{-1}$. So obviously, REcoM2 allows the Chl:C ratio to go down to values that are not encountered in the field. We therefore recommend the setting of a minimum threshold for future simulations.

3.3 Laws and Bannister experiment

Laws and Bannister (1980) studied in the laboratory how the Chl:C ratio in a diatom varied with growth rate, when the growth rate was determined by either light or nutrient (NH_4, NO_3 and PO_4) limitations, as described in section 3 of the state of the art. The aim of this analysis is to verify whether REcoM2 is in agreement with Laws and Bannister findings. In order to reproduce their experiment with the model, we used the equations associated with growth for diatoms, then for nanophytoplankton in REcoM2. We neglected any external influence, that is no grazing and no aggregation, so the only biomass losses were through respiration and excretion. The model was then integrated over a sufficient time scale to

reach equilibrium, that is, when phytoplankton internal composition is stable, even though biomass can still change. In other words, this balanced growth state is reached when the relative rate of change of the different cellular components are equal. The results are presented on Figure 10a and Figure 10b for diatoms and nanophytoplankton respectively. The trend is comparable in the two graphs, for both nutrient and light limitations. It appears that under light limitation and low growth rate, diatoms present a higher Chl:C ratio than nanophytoplankton. By comparing these graphs with Figure 1, we notice a high similitude, except at very low growth rate under light limitation. Indeed, in the Laws and Bannister experiment, the ratio increases with decreasing growth rate under light limitation, whereas in Figure 10, the ratio seems to decrease when the growth rate is lower than a certain value. A reason for that could be that some loss term is set too high. Our suspicions were pointing towards the Chl degradation rate, which is equal to 0.3 d^{-1} for both diatoms and nanophytoplankton in this model run. We decreased it progressively down to 0.05 d^{-1} and obtained the same curves as in Figure 1. REcoM2 is the only model among our set that considers a Chl degradation rate and this parameter is probably too high, see Appendix B1. This observation should be taken in consideration in future model runs and will be further investigated in subsection 3.5. Except for that, we can conclude that this run of REcoM2 seems to do a good job in representing the change of the Chl:C ratio with growth rate under light or nutrient limitations in balanced growth conditions.

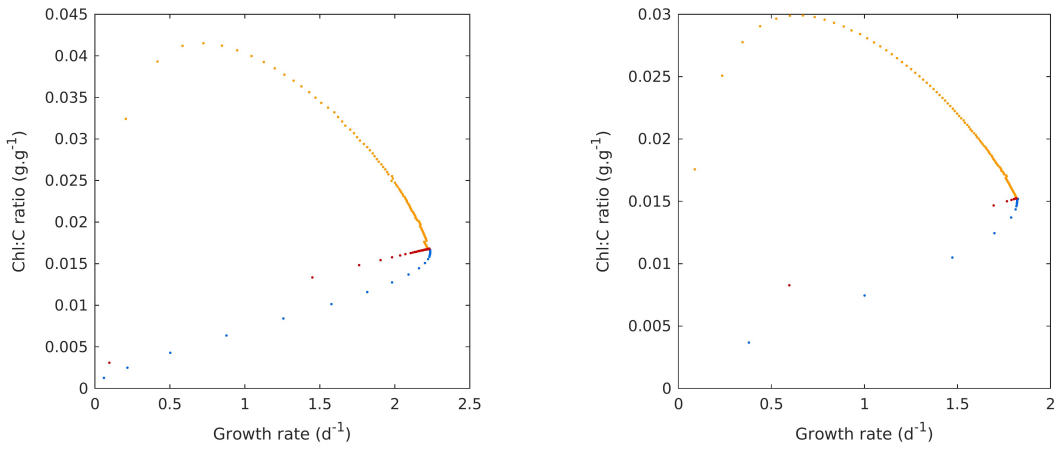

(a) Diatoms (b) Nanophytoplankton

Figure 10: Dependency of the Chl:C ratio on growth rate under light and nutrient limitations. The legend being Orange=Light-limited growth, Red=Fe-limited growth and Blue=N-limited growth. Note the different scale.

3.4 Hypothesis of unbalanced growth

The previous analysis raises the question "Is balanced growth ever reached in natural environments, especially in regions where there is very little growth?". While some models assume balanced growth conditions, REcoM2 does not, but allows for a separate evolution of Chl and C as in the model by Geider et al. (1998). Over long winters, REcoM2

decreases the biomass drastically under the ice, in polar regions, because of the lack of light. It is likely that the growth rate becomes so small that it would take longer than the winter duration for the cells to photoacclimate and reach equilibrium. In other words, respiration would be too high compared to production, preventing phytoplankton to reach steady state. This hypothesis, if true, could explain partly why the ratio is so low in winter in the Southern Ocean in REcoM2. In steady state conditions, the relative rate of change of Chl ($\frac{dChl/dt}{Chl}$) and C ($\frac{dC/dt}{C}$) should be equivalent and the difference of these relative changes should be close to zero. We therefore have to calculate this difference to verify the hypothesis that unbalanced growth conditions occur in REcoM2, especially in polar regions in winter. If the result is zero, it means that phytoplankton growth is balanced and if the result is significantly different from zero, then our hypothesis will be verified. We present the graphs obtained for both diatoms and nanophytoplankton in January (Figure 11) and July (Figure 12). Moreover, in order to know whether there is net growth, we also plotted the annual climatology of the relative rate of change of C (Appendix K). A positive value implies net growth whereas a negative value implies a decrease in biomass.

In January, for both diatoms and nanophytoplankton, the result of the difference is comprised between -0.25 and 0.25, but never exactly equal to zero, in most surface waters, which implies that balanced growth is more or less reached. In some regions, such as the northern Indian Ocean, the Equatorial Pacific and the central Atlantic, the result of the difference for diatoms can reach -1, and as the net growth rate is positive in these areas (Appendix K), it means that the relative rate of change of Chl is smaller than the relative rate of change of C. In these same regions, the result of the difference for nanophytoplankton is strongly positive, and as the net growth rate is positive as well (Appendix K), it means that the relative rate of change of Chl is much higher than the relative change of C.

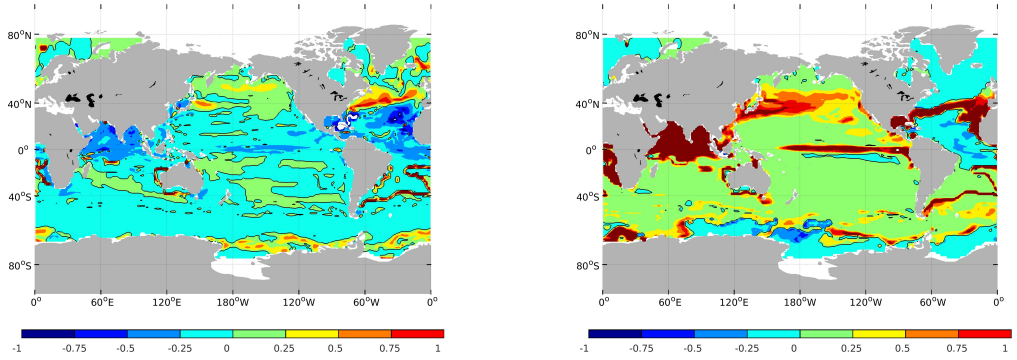

(a) Diatoms

(b) Nanophytoplankton

Figure 11: January climatology of the difference between the relative change of Chl and the relative change of C for diatoms and nanophytoplankton in surface waters simulated by REcoM2. A black contour line has been added to mark the limit between positive and negative values.

In July, the result of the difference for diatoms is strongly positive in the Ross and Weddell seas, where the net growth seems to be slightly negative (Appendix K). So the relative rate of change of Chl is positive. The result of the difference for nanophytoplankton is strongly positive in extended parts of the world oceans. Overall, approximate balanced growth conditions seem to be reached more often by diatoms than by nanophytoplankton, which often present really high relative rates of change of Chl compared to C.

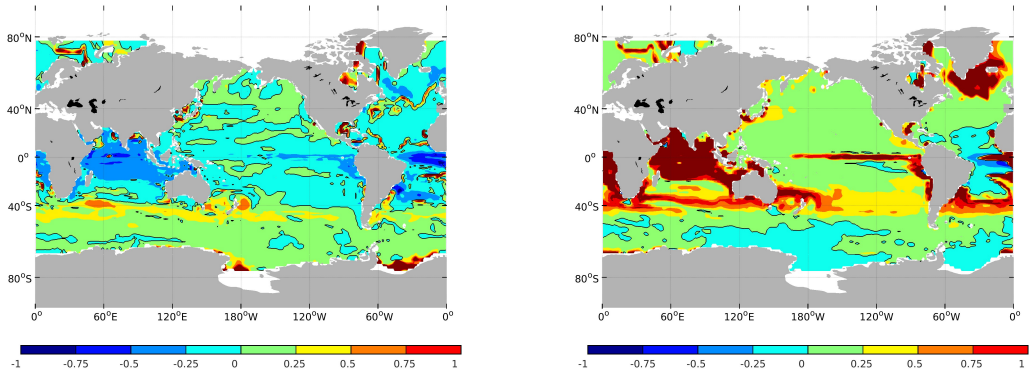

(a) Diatoms

(b) Nanophytoplankton

Figure 12: July climatology of the difference between the relative change of Chl and the relative change of C for diatoms and nanophytoplankton in surface waters simulated by REcoM2. A black contour line has been added to mark the limit between positive and negative values.

Many of the features seen in Figure 11 and Figure 12 are challenging to explain and would require a deeper analysis than was feasible within the time limits of this thesis. The main point we wanted to make in this subsection is that most models assume balanced growth and are therefore only valid under these restrictive conditions. However, in natural environments, balanced growth is probably rarely reached. Except for the model by Geider et al. (1998) which allows for an uncoupling of the physiological rates of change, and on which REcoM2 is based, very little is actually known on the behaviour of the Chl:C ratio under unbalanced growth conditions.

3.5 Parameter sensitivity

In this last analysis, we would like to carry out sensitivity runs on two specific parameters of REcoM2 to verify how they affect the Chl:C ratio. The first parameter is the Chl degradation rate. As we mentioned earlier, REcoM2 is the only model among our set to consider such a parameter, leading to different sink terms for C and Chl (see Appendix B1), while the other models usually consider a respiration rate instead of a degradation rate. The reason behind the use of this parameter in REcoM2 is mainly to obtain a good fit with Chl observations, so it might have been set inappropriately. However, Chl degradation has a true physiological significance as evidenced by the few studies on this topic (Hendry et al., 1987; Hörtensteiner, 1999; Matile et al., 1999). The different biochemical

reactions as well as the intermediary catabolites involved in Chl degradation and leading to non-fluorescent products are known in higher plants (Hörtensteiner, 1999). Chl breakdown has also been studied in *Chlorella* but the knowledge on the biochemical pathway is still limited (Hörtensteiner, 1999). What is far less investigated is the rate of this process in algae. Under steady state conditions the turnover of Chl can be quite fast, i.e. on the order of a few hours (Riper et al., 1979). But under non steady state conditions, which is often the case in natural environments, production and degradation of Chl can be uncoupled and then, Chl degradation can affect the net Chl concentration. The lack of literature on the topic makes it very difficult to assess the value of the Chl degradation rate used in REcoM2.

The second parameter we would like to test is the maximum Chl:N ratio. As REcoM2 is based on the model by Geider et al. (1998), the Chl synthesis rate is dependent on the N assimilation rate, see Appendix B1. A constant maximum Chl:N ratio is applied for conversion into Chl units. We therefore would like to investigate the impact of a change in this parameter on the Chl:C ratio.

The sensitivity runs were integrated over a short period, starting from the state of the initial run in 1995 (the initial run of REcoM2 was integrated from 1947). The parameters are modified in 1995 and the model is run until 2012. As we calculate the annual climatology of the Chl:C ratio for the 2000-2005 period as before, it means that the model has 5 years to adapt to this new parameterization. Five years are quite enough for the ecosystem part of the models to reach equilibrium, while nutrient and C distributions will still be quite close to the initial values. In total, we carried out four sensitivity runs for both diatoms and nanophytoplankton:

- The first sensitivity run has a degradation rate of Chl reduced from 0.3 to 0.05 d^{-1} (for both diatoms and nanophytoplankton)
- The second sensitivity run has a degradation rate of Chl reduced from 0.3 to 0 d^{-1} (for both diatoms and nanophytoplankton)
- The third sensitivity run has a maximum Chl:N ratio reduced from 0.315 to 0.21 mg Chl $(mmol\ N)^{-1}$ for nanophytoplankton and from 0.42 to 0.315 mg Chl $(mmol\ N)^{-1}$ for diatoms
- The fourth sensitivity run has a maximum Chl:N ratio increased from 0.315 to 0.42 mg Chl $(mmol\ N)^{-1}$ for nanophytoplankton and from 0.42 to 0.525 mg Chl $(mmol\ N)^{-1}$ for diatoms

The graphs obtained from the first sensitivity run are presented in Figure 13a and Figure 13b for diatoms and nanophytoplankton respectively. In Figure 13a, we notice that, except in the gyres, both the amplitude and the pattern of the Chl:C ratio have changed compared to the initial run. The areas that presented a high ratio in the initial run,

such as the northern Indian Ocean, the Equatorial Pacific and the western coast of Africa, present now an even higher ratio. But the global pattern has changed given that the ratio is notably higher in the Southern Ocean and at high northern latitudes. This is more in agreement with the pattern shown by the other models, except NOBM, in Figure 8. So the high Chl degradation rate in REcoM2 initial parameter set is probably partly responsible for the very low Chl:C ratios observed at high latitudes, as the low growth rate in winter can not keep up with such a loss. In Figure 13b, the Chl:C ratio increases everywhere, this time even in the gyres, which changes the global pattern. This is particularly obvious in the Southern Ocean, where the ratio is much higher than before.

The maps generated from the three remaining sensitivity runs can be found in Appendix L for both diatoms and nanophytoplankton. The second sensitivity run considers no Chl degradation, implying that the only Chl losses are through aggregation and grazing. The incredibly high values of the Chl:C ratio obtained for diatoms and nanophytoplankton, particularly in the gyres, are inconsistent with observations. This leads us to conclude that the hypothesis of no loss by degradation (or respiration as considered in other models) is erratic. Sensitivity runs 3 and 4 only affect the amplitude of the Chl:C ratio, but not its pattern. The Chl:C ratio increases with the maximum Chl:N ratio, leaving the pattern untouched. This means that the maximum Chl:N ratio can thus not explain the differences between REcoM2 and the other models.

Thanks to this last analysis, we can conclude that the Chl:C ratio in REcoM2 is quite sensitive to changes in the Chl degradation rate and less sensitive to changes in the maximum Chl:N ratio, which only result in a shift of the Chl:C ratio. In order to improve future simulations, an effort should be put in determining a more adapted Chl degradation rate given than this parameter seems to have a great influence on the Chl:C ratio in REcoM2 and is not well constrained from biological studies.

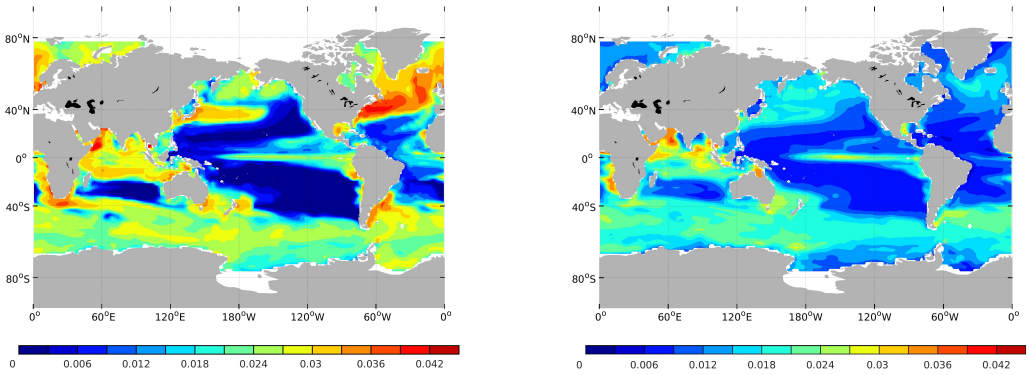

(a) Diatoms

(b) Nanophytoplankton

Figure 13: Annual climatology of the Chl:C ratio (mg mg^{-1}) for diatoms and nanophytoplankton in surface waters obtained with the first sensitivity run conducted with REcoM2.

Part V

Conclusion

As all kind of models, marine ecosystem models only provide a simplified representation of what is really happening in natural environments. Indeed, two main constraints stand in the way. Firstly, our knowledge on natural processes is often limited and secondly, even if we fully understood a system, the computational costs and time associated with its modelling would be incredibly high. Nevertheless, models allow us to approach this complex reality. They appear to be powerful tools to study biogeochemical cycles, and in particular, the carbon cycle, which is the center of growing attention in a context of global warming. They rapidly became an essential part of the decision process for policy makers regarding environmental management.

The number and complexity of marine ecosystem models have greatly increased over the last two decades and it has become necessary to compare them and evaluate their performance. By this present study, based on a large ensemble of marine ecosystem models, we hope to contribute to this joint effort aiming at model improvement. We focus on eight model simulations from MAREMIP and/or CMIP5, i.e. REcoM2, TOPAZ, MEM, NOBM, PlankTOM5.3, BEC, CNRM-PISCES and IPSL-PISCES, for the 2000-2005 period.

The first part of this work consisted in assessing the ability of the models to simulate Chl concentrations in surface oceans by comparing them with satellite observations. Globally, model simulations represent quite well the regional pattern of Chl annual climatology in the open ocean. Indeed, common features comprise very low Chl concentrations in the gyres, a tongue of higher Chl concentrations in the eastern Equatorial Pacific and average concentrations on the order of 0.5 mg m^{-3} elsewhere. Very high Chl concentrations observed in coastal regions, on the other hand, are not well simulated by models, partly due to their coarse resolution. Another source of discrepancies between satellite observations and model simulations arises from the fact that the annual climatology of Chl concentrations estimated from satellite observations is biased towards summer in high latitude regions.

The central part of this master thesis deals with the phytoplankton Chl:C ratio in model simulations. As C biomass is extremely difficult to measure *in situ*, Chl has rapidly become one of the reference proxies given its optical properties that can be easily measured on the field and remotely. A quantification of the phytoplankton Chl:C ratio is then needed to obtain estimations of marine primary production. However it is now commonly accepted that phytoplankton can regulate their cellular composition in order to maximise their growth rate under limiting or adverse environmental conditions through a process called acclimation (Geider et al., 1998). As a result, the phytoplankton Chl:C ratio is not constant and varies with ambient temperature, light and nutrient conditions. It is therefore essential to understand these variations in the ratio if we want to improve our estimations of primary

production, and this is where models may prove to be helpful. The eight model simulations used in this study have different ways of dealing with this ratio: MEM uses a constant ratio, the ratio in NOBM is only light-dependent, and the remaining models allow for a variable ratio (Chl is a diagnostic variable in TOPAZ and a prognostic one in the others). Nevertheless, all the model simulations agree on the fact that the slope of the linear regression between phytoplankton carbon and chlorophyll is a number smaller than 1.

Eventually, we focused on REcoM2, as this model behaves quite differently from the others regarding the annual climatology of the Chl:C ratio. We noticed three things. First, the Chl degradation rate is probably too high in this model run and should be decreased down to around 0.05 d^{-1} in future simulations. The second thing is that REcoM2 allows for very low minimum values of the Chl:C ratio that are not encountered in other models or in the field. Setting a minimum threshold would probably improve REcoM2 outputs. Eventually, an interesting feature about REcoM2 is that it can handle unbalanced growth conditions. Some of the other models are only valid under the hypothesis of balanced growth, which rarely happens in natural environments.

Some issues were encountered in the course of this study. Firstly, as ecosystem models are run with different ocean and atmospheric models, it is difficult to assess the percentage of variability attributed only to a specific ecosystem model. To achieve a proper comparison of ecosystem models, it would be interesting to run them with the same models and define the same initial conditions. A similar statement can be made for the structural equations. Indeed, each model uses its proper terms. It would make the comparison much easier if the same processes were written in the same way, and if the same variables had the same name. Ecosystem model comparison will be really efficient when the ecosystem model is the only thing that will differ from one simulation to another. Secondly, a more extensive database on the Chl:C ratio from field experiments would greatly help to improve model outputs. Unfortunately, the rare measurements are currently scattered across the literature or not made available. Thirdly, the model simulations used in this work have a coarse resolution, implying that some small scale processes are not taken into account. Increase the resolution would maybe reveal interesting patterns in the Chl:C ratio.

This analysis focus on the surface Chl:C ratio, however, as light decreases with depth and nutrients generally increase, it would be an interesting subject for a further study to investigate the depth dependency of the ratio in the models. Other analyses that would help to refine our understanding on the variability of the Chl:C ratio among model simulations comprise the investigation of the seasonal cycle, of the differences between PFTs and of non steady state conditions. Even though marine ecosystem modelling is quite a new field of expertise, it has already considerably increased our knowledge on biogeochemical cycles. We hope this present study brought some enlightenment on the variability of the phytoplankton Chl:C ratio and will contribute to improve our estimations of primary production and by this means, future climate projections.

Part VI
References

Articles

Aksnes, D. L. and Egge, J. K. (1991). A theoretical model for nutrient uptake in phytoplankton. *Marine Ecology Progress Series*, 70(1):65–72, doi:10.3354/meps070065.

Arrigo, K. R., van Dijken, G. L., and Bushinsky, S. (2008a). Primary production in the Southern Ocean, 1997–2006. *Journal of Geophysical Research*, 113, C08004, doi:10.1029/2007JC004551.

Arrigo, K. R., van Dijken, G. L., and Pabi, S. (2008b). Impact of a shrinking Arctic ice cover on marine primary production. *Geophysical Research Letters*, 35, L19603, doi:10.1029/2008GL035028.

Aumont, O. and Bopp, L. (2006). Globalizing results from ocean in situ iron fertilization studies. *Global Biogeochemical Cycles*, 20, GB2017, doi:10.1029/2005GB002591.

Beale, S. I. and Appleman, D. (1971). Chlorophyll synthesis in *Chlorella*: regulation by degree of light limitation of growth. *Plant physiology*, 47(2):230–235, doi:10.1104/pp.47.2.230.

Behrenfeld, M. J., Marañón, E., Siegel, D. A., and Hooker, S. B. (2002). Photoacclimation and nutrient-based model of light-saturated photosynthesis for quantifying oceanic primary production. *Marine Ecology Progress Series*, 228:103–117, doi:10.3354/meps228103.

Behrenfeld, M. J. and Milligan, A. J. (2013). Photophysiological Expressions of Iron Stress in Phytoplankton. *Annual Review of Marine Science*, 5:217–246, doi: 10.1146/annurev–marine–121211–172356.

Buitenhuis, E. T., Hashioka, T., and Quéré, C. L. (2013). Combined constraints on global ocean primary production using observations and models. *Global Biogeochemical Cycles*, 27(3):847–858, doi:10.1002/gbc.20074.

Chavez, F. P., Messié, M., and Pennington, J. T. (2011). Marine primary production in relation to climate variability and change. *Annual review of marine science*, 3:227–260, doi:10.1146/annurev.marine.010908.163917.

Cloern, J. E., Grenz, C., and Vidergar-Lucas, L. (1995). An empirical model of the phytoplankton chlorophyll : carbon ratio-the conversion factor between productivity and growth rate. *Limnology and Oceanography*, 40(7):1321–1326, doi:10.4319/lo.1995.40.7.1313.

Cullen, J. J. (1982). The deep chlorophyll maximum: comparing vertical profiles of chlorophyll *a*. *Journal of Fisheries and Aquatic Sciences*, 39(5):791–803, doi:10.1139/f82–108.

Cullen, J. J. and Lewis, M. R. (1988). The kinetics of algal photoadaptation in the context of vertical mixing. *Journal of Plankton Research*, 10(5):1039–1063. doi:10.1093/plankt/10.5.1039.

de Baar, H. J. W. (1994). von Liebig's Law of the Minimum and plankton ecology (1899-1991). *Progress in Oceanography*, 33(4):347–386, doi:10.1016/0079–6611(94)90022–1.

Droop, M. R. (1983). 25 Years of Algal Growth Kinetics A Personal View. *Botanica Marina*, 26(3):99–112, doi:10.1515/botm.1983.26.3.99.

Dunne, J. P., Armstrong, R. A., Gnnadesikan, A., and Sarmiento, J. L. (2005). Empirical and mechanistic models for the particle export ratio. *Global Biogeochemical Cycles*, 19, GB4026, doi:10.1029/2004GB002390.

Dunne, J. P., John, J. G., Shevliakova, S., Stouffer, R. J., Krasting, J. P., Malyshev, S. L., Milly, P. C. D., Sentman, L. T., Adcroft, A. J., Cooke, W., Dunne, K. A., Griffies, S. M., Hallberg, R. W., Harrison, M. J., Levy, H., Wittenberg, A. T., Phillips, P. J., and Zadeh, N. (2013). GFDL's ESM2 global coupled climate-carbon earth system models. Part II: Carbon system formulation and baseline simulation characteristics. *Journal of Climate*, 26(7):2247–2267, doi:10.1175/JCLI–D–12–00150.1.

Eppley, R. W. (1972). Temperature and phytoplankton growth in the sea. *Fishery Bulletin*, 70(4):1063–1085.

Falkowski, P. G., Dubinsky, Z., and Wyman, K. (1985). Growth-irradiance relationships in phytoplankton. *Limnology and Oceanography*, 30(2):311–321, doi:10.4319/lo.1985.30.2.0311.

Falkowski, P. G., Katz, M. E., Knoll, A. H., Quigg, A., Raven, J. A., Schofield, O., and Taylor, F. J. R. (2004). The evolution of modern eukaryotic phytoplankton. *Science*, 35(5682):354–360, doi:10.1126/science.1095964.

Falkowski, P. G. and LaRoche, J. (1991). Acclimation to spectral irrandiance in algae. *Journal of Phycology*, 27(1):8–14, doi:10.1111/j.0022–3646.1991.00008.x.

Falkowski, P. G. and Owens, T. G. (1980). Light-Shade Adaptation : two strategies in marine phytoplankton. *Plant physiology*, 66(4):592–595, doi:10.1104/pp.66.4.592.

Field, C. B. (1998). Primary Production of the Biosphere: Integrating Terrestrial and Oceanic Components. *Science*, 281(5374):237–240, doi:10.1126/science.281.5374.237.

Geider, R. and La Roche, J. (2002). Redfield revisited: variability of C:N:P in marine microalgae and its biochemical basis. *European Journal of Phycology*, 37(1):1–17, doi:10.1017/S0967026201003456.

Geider, R. J. (1987). Light and temperature dependence of the carbon to chlorophyll *a* ratio in microalgae and cyanobacteria : implications for physiology and growth of phytoplankton. *New Phytologist*, 106(1):1–34, doi:10.1111/j.1469–8137.1987.tb04788.x.

Geider, R. J., MacIntyre, H. L., and Kana, T. M. (1996). A dynamic model of photoadaptation in phytoplankton. *Limnology and Oceanography*, 41(1):1–15, doi:10.4319/lo.1996.41.1.0001.

Geider, R. J., MacIntyre, H. L., and Kana, T. M. (1997). Dynamic model of phytoplankton growth and acclimation: responses of the balanced growth rate and the chlorophyll *a*:carbon ratio to light, nutrient-limitation and temperature. *Marine Ecology Progress Series*, 148:187–200, doi:10.3354/meps148187.

Geider, R. J., MacIntyre, H. L., and Kana, T. M. (1998). A dynamic regulatory model of phytoplanktonic acclimation to light, nutrients and temperature. *Limnology and Oceanography*, 43(4):679–694, doi:10.4319/lo.1998.43.4.0679.

Graff, J. R., Westberry, T. K., Milligan, A. J., Brown, M. B., Dall'Olmo, G., van Dongen-Vogels, V., Reifel, K. M., and Behrenfeld, M. J. (2015). Analytical phytoplankton carbon measurements spanning diverse ecosystems. *Deep Sea Research Part I: Oceanographic Research Papers*, 102:16–25, doi:10.1016/j.dsr.2015.04.006.

Gregg, W. W. and Casey, N. W. (2007). Modeling coccolithophores in the global oceans. *Deep-Sea Research Part II: Topical Studies in Oceanography*, 54(5–7):447–477, doi:10.1016/j.dsr2.2006.12.007.

Hauck, J., Völker, C., Wang, T., Hoppema, M., Losch, M., and Wolf-Gladrow, D. A. (2013). Seasonally different carbon flux changes in the Southern Ocean in response to the southern annular mode. *Global Biogeochemical Cycles*, 27(4):1236–1245, doi:10.1002/2013GB004600.

Hendry, G. A. F., Houghton, J. D., and Brown, S. B. (1987). Tansley Review No. 11. The degradation of chlorophyll–a biological enigma. *New Phytologist*, 107(2):255–302.

Hörtensteiner, S. (1999). Chlorophyll breakdown in higher plants and algae. *Cellular and Molecular Life Sciences CMLS*, 56(3–4):330–347, doi:10.1007/s000180050434.

Hoskisson, P. A. and Hobbs, G. (2005). Continuous culture - Making a comeback? *Microbiology*, 151:3153–3159, doi:10.1099/mic.0.27924–0.

Laufkötter, C., Vogt, M., Gruber, N., Aita-Noguchi, M., Aumont, O., Bopp, L., Buitenhuis, E., Doney, S. C., Dunne, J., Hashioka, T., Hauck, J., Hirata, T., John, J., Le Quéré, C., Lima, I. D., Nakano, H., Seferian, R., Totterdell, I., Vichi, M., and Völker, C. (2015). Drivers and uncertainties of future global marine primary production in marine ecosystem models. *Biogeosciences Discussions*, 12:3731–3824, doi:10.5194/bgd–12–3731–2015.

Laws, E. A. and Bannister, T. T. (1980). Nutrient- and light-limited growth of Thalassiosira fluviatilis in continuous culture, with implications for phytoplankton growth in the ocean. *Limnology and Oceanography*, 25(3):457–473, doi:10.4319/lo.1980.25.3.0457.

Le Quéré, C., Harrison, S. P., Prentice, I. C., Buitenhuis, E. T., Aumont, O., Bopp, L., Claustre, H., Cotrim Da Cunha, L., Geider, R., Giraud, X., Klaas, C., Kohfeld, K. E., Legendre, L., Manizza, M., Platt, T., Rivkin, R. B., Sathyendranath, S., Uitz, J., Watson, A. J., and Wolf-Gladrow, D. (2005). Ecosystem dynamics based on plankton functional types for global ocean biogeochemistry models. *Global Change Biology*, 11(11):2016–2040, doi:10.1111/j.1365–2486.2005.1004.x.

Liebig, J. (1840). *Chemistry and its Applications to Agriculture and Physiology: on Chemical Processes in the Nutrition of Vegetables*. Taylor and Walton, London.

Marcus, N. H. and Boero, F. (1998). Minireview: The importance of benthic-pelagic coupling and the forgotten role of life cycles in coastal aquatic systems. *Limnology and Oceanography*, 43(5):763–768, doi:10.4319/lo.1998.43.5.0763.

Matile, P., Hörtensteiner, S., and Thomas, H. (1999). Chlorophyll degradation. *Annual Review of Plant Physiology and Plant Molecular Biology*, 50:67–95, doi:10.1146/annurev.arplant.50.1.67.

Moore, J. K., Lindsay, K., Doney, S. C., Long, M. C., and Misumi, K. (2013). Marine ecosystem dynamics and biogeochemical cycling in the community earth system model [CESM1(BGC)]: Comparison of the 1990s with the 2090s under the RCP4.5 and RCP8.5 scenarios. *Journal of Climate*, 26:9291–9312, doi:10.1175/JCLI–D–12–00566.1.

Myers, J. (1946). Influence of light intensity on photosynthetic characteristics of *Chlorella*. *The Journal of General Physiology*, 29(6):429–440, doi:10.1085/jgp.29.6.429.

Pabi, S., van Dijken, G. L., and Arrigo, K. R. (2008). Primary production in the Arctic Ocean, 1998-2006. *Journal of Geophysical Research: Oceans*, 113, C08005, doi:10.1029/2007JC004578.

Platt, T., Gallegos, C., and Harrison, W. (1980). Photoinhibition of photosynthesis in natural assemblages of marine phytoplankton. *Journal of Marine Research*, 38:687–701.

Redfield, A. C. (1958). The biological control of chemical factors in the environment. *American Scientist*, 46(3):205–221, doi:10.5194/bg–11–1599–2014.

Riper, D. M., Owens, T. G., and Falkowski, P. G. (1979). Chlorophyll turnover in *Skeletonema costatum*, a marine plankton diatom. *Plant Physiology*, 64(1):49–54, doi:http://dx.doi.org/10.1104/pp.64.1.49.

Saito, M. A., Goepfert, T. J., and Ritt, J. T. (2008). Some thoughts on the concept of colimitation: Three definitions and the importance of bioavailability. *Limnology and Oceanography*, 53(1):276–290, doi:10.4319/lo.2008.53.1.0276.

Sathyendranath, S., Stuart, V., Nair, A., Oka, K., Nakane, T., Bouman, H., Forget, M. H., Maass, H., and Platt, T. (2009). Carbon-to-chlorophyll ratio and growth rate of phytoplankton in the sea. *Marine Ecology Progress Series*, 383:73–84, doi:10.3354/meps07998.

Shigemitsu, M., Okunishi, T., Nishioka, J., Sumata, H., Hashioka, T., Aita, M. N., Smith, S. L., Yoshie, N., Okada, N., and Yamanaka, Y. (2012). Development of a one-dimensional ecosystem model including the iron cycle applied to the Oyashio region, western subarctic Pacific. *Journal of Geophysical Research: Oceans*, 117, C06021, doi:10.1029/2011JC007689.

Shuter, B. (1979). A model of physiological adaptation in unicellular algae. *Journal of theoretical biology*, 78:519–552, doi:10.1016/0022–5193(79)90189–9.

Smith, S. L., Yamanaka, Y., Pahlow, M., and Oschlies, A. (2009). Optimal uptake kinetics: Physiological acclimation explains the pattern of nitrate uptake by phytoplankton in the ocean. *Marine Ecology Progress Series*, 384:1–12, doi:10.3354/meps08022.

Sommer, U. (1991). A Comparison of the Droop and the Monod Models of Nutrient Limited Growth Applied to Natural Populations of Phytoplankton. *Functional Ecology*, 5(4):535–544, doi:10.2307/2389636.

Steinacher, M., Joos, F., Frölicher, T. L., Bopp, L., Cadule, P., Doney, S. C., Gehlen, M., Schneider, B., and Segschneider, J. (2010). Projected 21st century decrease in marine productivity: a multi-model analysis. *Biogeosciences*, 7:979–1005, doi:10.5194/bg–7–979–2010.

Strzepek, R. F. and Harrison, P. J. (2004). Photosynthetic architecture differs in coastal and oceanic diatoms. *Nature*, 431:689–692 , doi:10.1038/nature02954.

Taylor, K. E. (2001). Summarizing multiple aspects of model performance in a single diagram. *Journal of Geophysical Research*, 106(D7):7183–7192, doi:10.1029/2000JD900719.

Websites

OCMIP Ocean Carbon-Cycle Model Intercomparison Project, [online], Available: http://ocmip5.ipsl.jussieu.fr/OCMIP/ [Accessed July 14th, 2015].

CMIP5 Coupled Model Intercomparison Project 5 - Overview, [online], Available: http://cmip-pcmdi.llnl.gov/cmip5/index.html?submenuheader=0 [Accessed July 15th, 2015].

CMIP5 Coupled Model Intercomparison Project 5 - All publications, [online], Available: http://cmip.llnl.gov/cmip5/publications/allpublications [Accessed July 15th, 2015].

MAREMIP MARine Ecosystem Model Intercomparison Project, [online], Available: http://pft.ees.hokudai.ac.jp/maremip/index.shtml [Accessed July 15th, 2015].

Ocean Color-CCI, [online], Available: http://www.oceancolour.org/ [Accessed March 9th-17th, 2015].

ESA Ocean colour, [online], Available: http://www.esa-oceancolour-cci.org/ [Accessed April 28th, 2015].

Climate Data Operators, [online], Available: https://code.zmaw.de/projects/cdo [Accessed March 10th, 2015].

Earth System Grid Federation, [online], Available: http://esgf-node.ipsl.fr/esgf-web-fe/ [Accessed March 4th, 2015].

Part VII
Appendices

Appendix A: Characteristics of the eight model simulations used in this work, extended from Laufkötter et al. (2015).

Appendix B: Equations describing the source and sink terms for C and Chl in the eight model simulations used in this work.

Appendix C: Taylor diagrams showing the correspondence between model simulations and satellite observations with regard to typical monthly climatologies of Chl in surface waters.

Appendix D: Annual climatology of averaged Chl as a function of latitude computed for satellite observations and model simulations, modified by setting a maximum threshold for Chl of 5 $mg.m^{-3}$ and by applying the same bias as in satellite observations to model outputs.

Appendix E: January climatology of the Chl:C ratio ($mg.mg^{-1}$) in surface waters from model simulations.

Appendix F: July climatology of the Chl:C ratio ($mg.mg^{-1}$) in surface waters from model simulations.

Appendix G: Latitudinal behaviour of the C:Chl ratio.

Appendix H: Annual climatology of C versus Chl in surface waters from model simulations.

Appendix I: Distribution of the dominant limiting nutrient for diatoms in surface waters from model simulations.

Appendix J: Distribution of the dominant limiting nutrient for nanophytoplankton in surface waters from model simulations.

Appendix K: January and July climatologies of the relative change of C for diatoms and nanophytoplankton in surface waters simulated by REcoM2.

Appendix L: Initial model run and sensitivity runs on the annual climatology of the Chl:C ratio ($mg\ mg^{-1}$) in surface waters for diatoms and nanophytoplankton in REcoM2.

Appendix A: Characteristics of the eight model simulations used in this work, extended from Laufkötter et al. (2015). Fixed Redfield (R) or variable (V) ratios are used for the production of organic matter.

Ecosystem model	Reference	Atmospheric forcing	Ocean model	Coupling	PFTs	Nutrients	Stoichiometry
REcoM2	Hauck et al. (2013)	MIROC5	MITgcm	Ocean only	Diatoms Nanophytoplankton	NO_3,SiO_4,Fe	V(C,N,Si,Chl),(C:Fe) fix
PISCES	Aumont and Bopp (2006)	CNRM-CM5	NEMO	Fully coupled	Diatoms Nanophytoplankton	NO_3,NH_4,PO_4,SiO_4,Fe	R(C:N:P),V(Si,Chl,Fe)
TOPAZ	Dunne et al. (2010)	GFDL-ESM2M	MOM	Fully coupled	Diatoms Nanophytoplankton Large phytoplankton Diazotrophic phytoplankton	NO_3,NH_4,PO_4,SiO_4,Fe	R(C:N),V(P,Si,Chl,Fe)
PISCES	Aumont and Bopp (2006)	IPSL-CM5A-LR	NEMO	Fully coupled	Diatoms Nanophytoplankton	NO_3,NH_4,PO_4,SiO_4,Fe	R(C:N:P),V(Si,Chl,Fe)
MEM	Shigemitsu et al. (2012)	MIROC5	MRI.COM	Ocean only	Diatoms Nanophytoplankton	NO_3,NH_4,SiO_4,Fe	R(C:N),(C:Chl) fix (Si:N,Fe:N) optimized
NOBM	Gregg and Casey (2007)	NCEPR	NOBM	Ocean only	Diatoms Nanophytoplankton Coccolithophores Cyanobacteria	NO_3,NH_4,SiO_4,Fe	R(C:N:Si),V(Chl),(C:Fe) fix
PlankTOM5.3	Buitenhuis et al. (2013)	IPSL-CM5A-LR	NEMO	Ocean only	Diatoms Nanophytoplankton Coccolithophores	NO_3,SiO_4,Fe	R(C:N),V(Si,Chl,Fe)
BEC	Moore et al. (2013)	CESM1	POP	Fully coupled	Diatoms Nanophytoplankton Diazotrophic phytoplankton	NO_3,NH_4,PO_4,SiO_4,Fe	R(C:N:P),V(Si,Chl,Fe)

Appendix B: Equations describing the source and sink terms for C and Chl in the eight model simulations used in this work.

In this appendix, we present equations of the sources and sinks term for C and Chl. Detailed equations and parameters can be found in the reference papers (REcoM2, Hauck et al. (2013); TOPAZ, Dunne et al. (2013); MEM, Shigemitsu et al. (2012); NOBM, Gregg and Casey (2007); PlankTOM5.3, Buitenhuis et al. (2013); BEC, Moore et al. (2013); PISCES, Aumont and Bopp (2006)).

Symbol	**Meaning**
i	Phytoplankton type
C	Carbon biomass
Chl	Chlorophyll concentration
μ	Photosynthetic rate
θ	Intracellular ratio
I_{PAR}	Photosynthetically active radiation
α	Initial slope of the P-I curve

Table 1: General symbols used in the simplified model equations

B1 REcoM2

Sources and sinks of carbon

$$S(C^i) = \underbrace{\mu^i \times C^i}_{\text{Photosynthesis}} \underbrace{- \epsilon_C^i \times f_{lim}^i \times C^i}_{\text{Loss by excretion}} - \underbrace{r^i \times C^i}_{\text{Loss by respiration}} - \underbrace{g \times C^i}_{\text{Loss by aggregation}} - \underbrace{\frac{1}{\theta_{N/C}^i} \times G^i}_{\text{Loss by grazing}}$$

Sources and sinks of chlorophyll

$$S(Chl^i) = \underbrace{s^i \times C^i}_{\text{Chl synthesis}} - \underbrace{d_{Chl}^i \times Chl^i}_{\text{Loss by degradation}} - \underbrace{g \times Chl^i}_{\text{Loss by aggregation}} \underbrace{- G^i \times \theta_{Chl/N}^i}_{\text{Loss by grazing}}$$

$$s^i = a_N^i \times \theta_{Chl/N}^{i\,max} \times \underbrace{min\left(1, \frac{\mu^i}{\alpha^i \times \theta_{Chl/C}^i \times PAR}\right)}_{\substack{\text{Regulation term reflecting the ratio} \\ \text{of energy assimilated to energy absorbed}}}$$

Symbol	Meaning
ϵ_C	Excretion rate
f_{lim}	Function limiting N assimilation
r	Respiration rate
g	Aggregation rate
G	Relative contribution of grazing
s	Chl synthesis rate
d_{Chl}	Chl degradation rate
a_N	C-specific N assimilation rate

Table 2: Symbols specific to REcoM2

B2 PISCES

Sources and sinks of carbon

$$S(C^i) = \underbrace{\mu^i \times C^i}_{\text{Photosynthesis}} - \underbrace{\delta^i \times \mu^i \times C^i}_{\text{Loss by excretion}} - \underbrace{m^i \times \frac{C^i}{K^i + C^i} \times C^i}_{\text{Loss by mortality}} - \underbrace{w_p^i \times (C^i)^2}_{\text{Loss by aggregation}} - \underbrace{g^Z(C^i) \times Z}_{\text{Loss by grazing}} - \underbrace{g^M(C^i) \times M}_{\text{Loss by grazing}}$$

Sources and sinks of chlorophyll

$$S(Chl^i) = \underbrace{\rho^i_{Chl} \times \mu^i \times C^i}_{\text{Chl synthesis}} - \underbrace{\delta^i \times \rho^i_{Chl} \times \mu^i \times C^i}_{\text{Loss by excretion}} - \underbrace{m^P \times \frac{C^i}{K^i + C^i} \times Chl^i}_{\text{Loss by mortality}} - \underbrace{w_p^i \times C^i \times Chl^i}_{\text{Loss by aggregation}} - \underbrace{g^Z(C^i) \times \theta^i_{Chl/C} \times Z}_{\text{Loss by grazing}} - \underbrace{g^M(C^i) \times \theta^i_{Chl/C} \times M}_{\text{Loss by grazing}}$$

$$\rho^i_{Chl} = \theta^{\text{i max}}_{Chl/C} \times \frac{144 \times \mu^i \times C^i}{\alpha^i \times I_{PAR} \times Chl^i}$$

Symbol	Meaning
δ	Fraction excreted
m	Mortality rate
K	Half saturation constant for mortality
w_p	Aggregation term
$g^Z(C^i)$	Grazing by microzooplankton on phytoplankton
Z	Microzooplankton biomass
$g^M(C^i)$	Grazing by mesozooplankton on phytoplankton
M	Mesozooplankton biomass
ρ	Ratio of energy assimilated to energy absorbed

Table 3: Symbols specific to PISCES

B3 TOPAZ

Sources and sinks of carbon

In TOPAZ, they calculate the source and sink term for N biomass and then convert it to C using a fixed Redfield ratio. The only N-loss is through grazing.

Representation of chlorophyll

$$\theta^i_{Chl/C,min} = max(0.0, \theta^{nolim}_{Chl/C,min} - \theta^{lim}_{Chl/C,min}) \times N^i_{lim} + \theta^{lim}_{Chl/C,min}$$

$$\theta^i_{Chl/C} = \frac{\theta^i_{Chl/C,max} - \theta^i_{Chl/C,min}}{1.0 + (\theta^i_{Chl/C,max} - \theta^i_{Chl/C,min}) \times \alpha^i \times I_{mem} \times 0.5 \times \frac{1}{\mu^i_{max}}} + \theta^i_{Chl/C,min}$$

$$Chl = \theta_{C/N} \times 12 \times 10^6 \times (\theta^{small}_{Chl/C} \times [N]^{small} + \theta^{large}_{Chl/C} \times [N]^{large} + \theta^{diazo}_{Chl/C} \times [N]^{diazo})$$

Symbol	Meaning
θ_{min}	Minimum ratio
θ_{max}	Maximum ratio
θ^{nolim}_{min}	Minimum ratio without nutrient limitation
θ^{lim}_{min}	Minimum ratio under nutrient limitation
I_{mem}	Memory of irradiance over 24 hours
$[N]$	N concentration
N_{lim}	Nutrient limitation
μ_{max}	Maximum growth rate at 0 °C

Table 4: Symbols specific to TOPAZ

B4 MEM

Sources and sinks of carbon

$$S(C^i) = \underbrace{\mu^i \times C^i}_{\text{Photosynthesis}} - \underbrace{R^i \times e^{k_R^i \times T} \times C^i}_{\text{Loss by respiration}} - \underbrace{\gamma^i \times \mu^i \times C^i}_{\text{Loss by excretion}} - \underbrace{M^i \times e^{k_M^i \times T} \times (C^i)^2}_{\text{Loss by mortality}}$$
$$- \underbrace{\Sigma^j G_{i,max}^j \times max(0, 1 - e^{\lambda(C_j^{i*} - C^i)}) \times e^{k_G^j \times T} \times Z^j}_{\text{Loss by grazing}}$$

Representation of chlorophyll

$\theta^{nano} = 0.008$

$\theta^{diat} = 0.02$

Symbol	Meaning
R	Respiration rate
k_R	Temperature coefficient for respiration
T	Temperature
γ	Ratio of extracellular excretion to photosynthesis
M	Mortality rate
k_M	Temperature coefficient for mortality
$G_{i,max}^j$	Max. rate of grazing of zooplankton j on phytoplankton i
λ	Ivlev constant
C_j^{i*}	Threshold value for grazing on phytoplankton i
k_G	Temperature coefficient for grazing
Z^j	Zooplankton j biomass

Table 5: Symbols specific to MEM

B5 NOBM

Sources and sinks of carbon

$$S(C^i) = \underbrace{\mu^i \times C^i}_{\text{Photosynthesis}} - \underbrace{\nabla(w_s^i) \times C^i}_{\text{Loss by sinking}} - \underbrace{\delta \times C^i}_{\text{Loss by excretion}} - \underbrace{\Omega \times C^i}_{\text{Loss by respiration}} - \underbrace{\gamma \times H}_{\text{Loss by grazing}} - \underbrace{\kappa \times C^i}_{\text{Loss by mortality}}$$

Representation of chlorophyll

Chl concentrations are calculated from the C:Chl ratio, which is not constant (Gregg and Casey, 2007). The authors use three different light states, a low (50 μmol quanta m^{-2} s^{-1}), a medium (150 μmol quanta m^{-2} s^{-1}) and a high one (200 μmol quanta m^{-2} s^{-1}). They attribute a different C:Chl ratio to each of these light states, based on laboratory studies, in order to account for photoadaptation: 25, 50 and 80 g g^{-1} respectively. Then, the ratios are linearly interpolated for irradiances falling between the three reference light levels.

Symbol	Meaning
w_s	Vector sinking rate of phytoplankton at 31 °C
δ	Excretion fraction
Ω	Respiration fraction
γ	Grazing rate
H	Zooplankton biomass
κ	Mortality rate

Table 6: Symbols specific to NOBM

B6 PlankTOM5.3

Sources and sinks of carbon

$$S(C^i) = \underbrace{\mu^i \times C^i}_{\text{Photosynthesis}} - \underbrace{d \times \mu^i \times C^i}_{\text{Loss by excretion}} - \underbrace{w^i \times C^i \times C^i}_{\substack{\text{Loss by respiration,} \\ \text{aggregation, mortality}}} - \underbrace{\Sigma^j g^i_{Z^j} \times Z^j \times C^i}_{\text{Loss by grazing}}$$

Sources and sinks of chlorophyll

$$S(Chl^i) = \underbrace{s^i \times C^i}_{\text{Chl synthesis}} - \underbrace{d \times s^i \times C^i}_{\text{Loss by excretion}} - \underbrace{w^i \times C^i \times Chl^i}_{\substack{\text{Loss by respiration,} \\ \text{aggregation, mortality}}} - \underbrace{\Sigma^j g^i_{Z^j} \times Z^j \times Chl^i}_{\text{Loss by grazing}}$$

$$s^i = \left(\mu^i_{max} \times \left(1 - exp\left(\frac{-\alpha^i \times \theta^i_{Chl/C} \times I_{PAR}}{\mu^i_{max}}\right)\right)\right)^2 \times \frac{\theta^i_{Chl/C,max}}{-\alpha^i \times \theta^i_{Chl/C} \times I_{PAR}}$$

Symbol	Meaning
d	Excretion fraction
w^i	Total loss rate
$g^i_{Z^j}$	Grazing rate of zooplankton Z^j on phytoplankton i
Z^j	Zooplankton biomass

Table 7: Symbols specific to PlankTOM5.3

B7 BEC

Sources and sinks of carbon

$$S(C^i) = \underbrace{\mu^i \times C^i}_{\text{Photosynthesis}} \underbrace{- u^i_{max} \times T_f \times \frac{(C^i)^2}{(C^i)^2 + g^2} \times Z}_{\text{Loss by grazing}} - \underbrace{m^i \times C^i}_{\text{Loss by mortality}}$$
$$- \underbrace{min(a^i_{max} \times C^i, p^i \times (C^i)^2)}_{\text{Loss by aggregation}}$$

Sources and sinks of chlorophyll

$$S(Chl^i) = \underbrace{\frac{\rho^i_{Chl} \cdot \mu^i \times \theta_{N/C}}{\theta^i_{Chl/C}} \times Chl^i}_{\text{Chl synthesis}} \underbrace{- u^i_{max} \times T_f \times \frac{(C^i)^2}{(C^i)^2 + g^2} \times Z \times \theta^i_{Chl/C}}_{\text{Loss by grazing}}$$
$$\underbrace{- m^i \times C^i \times \theta^i_{Chl/C}}_{\text{Loss by mortality}} \underbrace{- min(a^i_{max} \times C^i, p^i \times (C^i)^2) \times \theta^i_{Chl/C}}_{\text{Loss by aggregation}}$$

$$\rho^i_{Chl} = \theta^i_{Chl/N,max} \times \frac{\mu^i}{\alpha^i \times \theta^i_{Chl/C} \times I_{PAR}}$$

Symbol	Meaning
u_{max}	Max. zooplankton growth rate on phytoplankton i
T_f	Temperature function
Z	Zooplankton biomass
g	Zooplankton grazing coefficient
m	Linear mortality rate
a_{max}	Maximum aggregation rate
p	Quadratic mortality rate

Table 8: Symbols specific to BEC

Appendix C: Taylor diagrams showing the correspondence between model simulations and satellite observations with regard to typical monthly climatologies of Chl in surface waters. A=Observations, B=REcoM2, C=CNRM-PISCES, D=TOPAZ, E=IPSL-PISCES, F=MEM, G=NOBM, H=PlankTOM5.3, I=BEC.

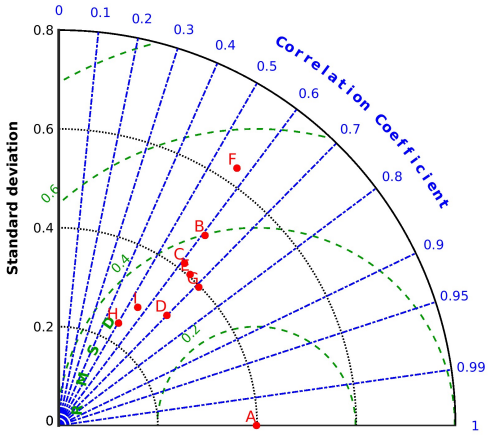

(a) January

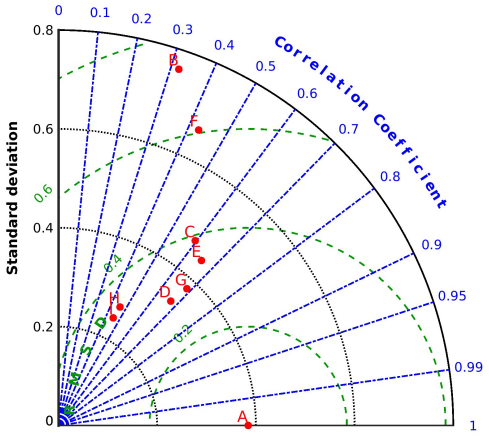

(b) March

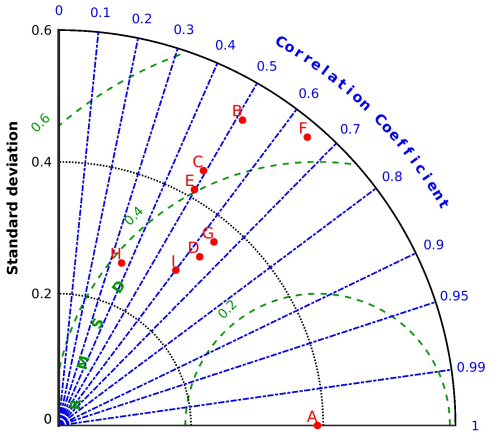

(c) July

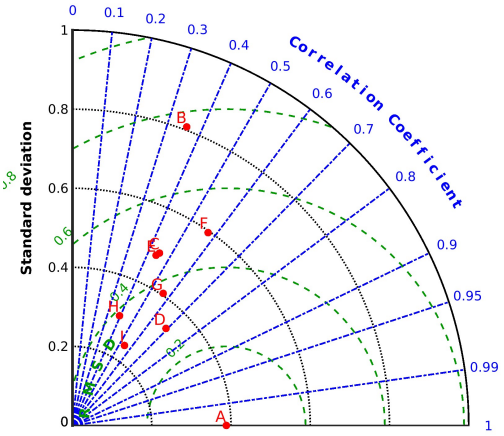

(d) September

Appendix D: Annual climatology of averaged Chl as a function of latitude computed for satellite observations and model simulations, modified by setting a maximum threshold for Chl of 5 mg.m^{-3} and by applying the same bias as in satellite observations to model outputs. Note the different scale for the two plots.

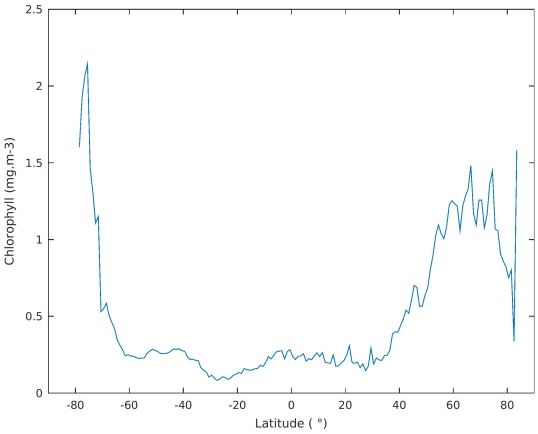

(e) Satellite observations

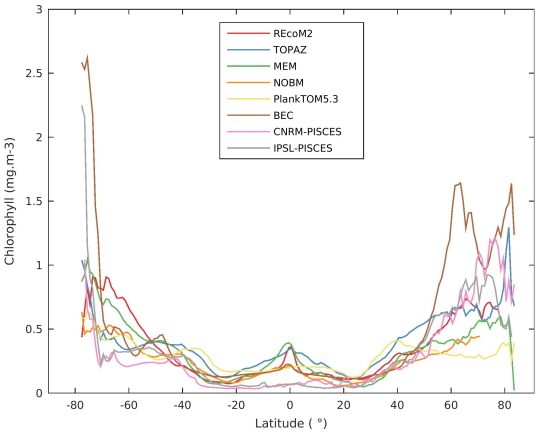

(f) Model simulations

Appendix E: January climatology of the Chl:C ratio (mg mg^{-1}) in surface waters from model simulations.

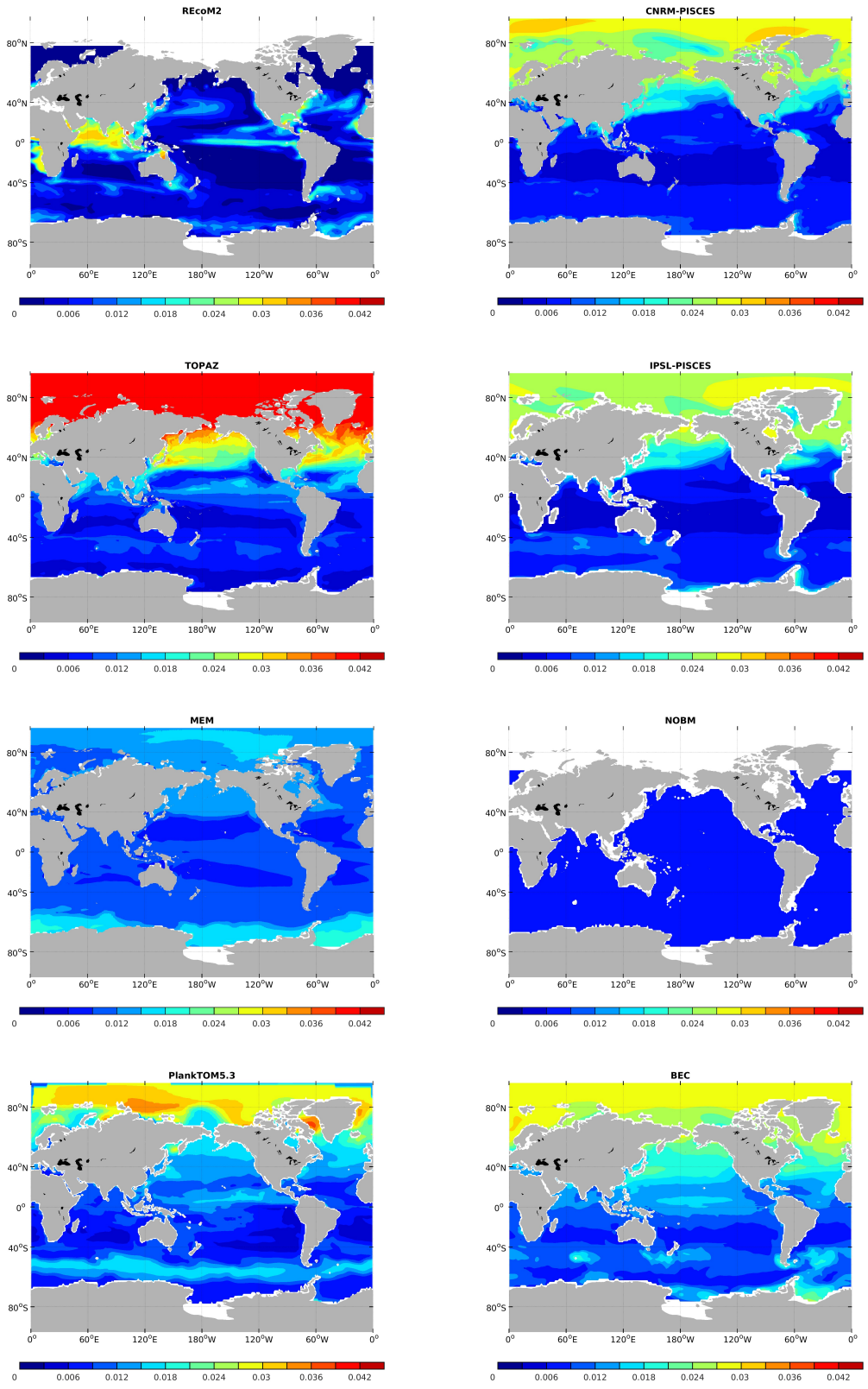

Appendix F: July climatology of the Chl:C ratio (mg mg^{-1}) in surface waters from model simulations.

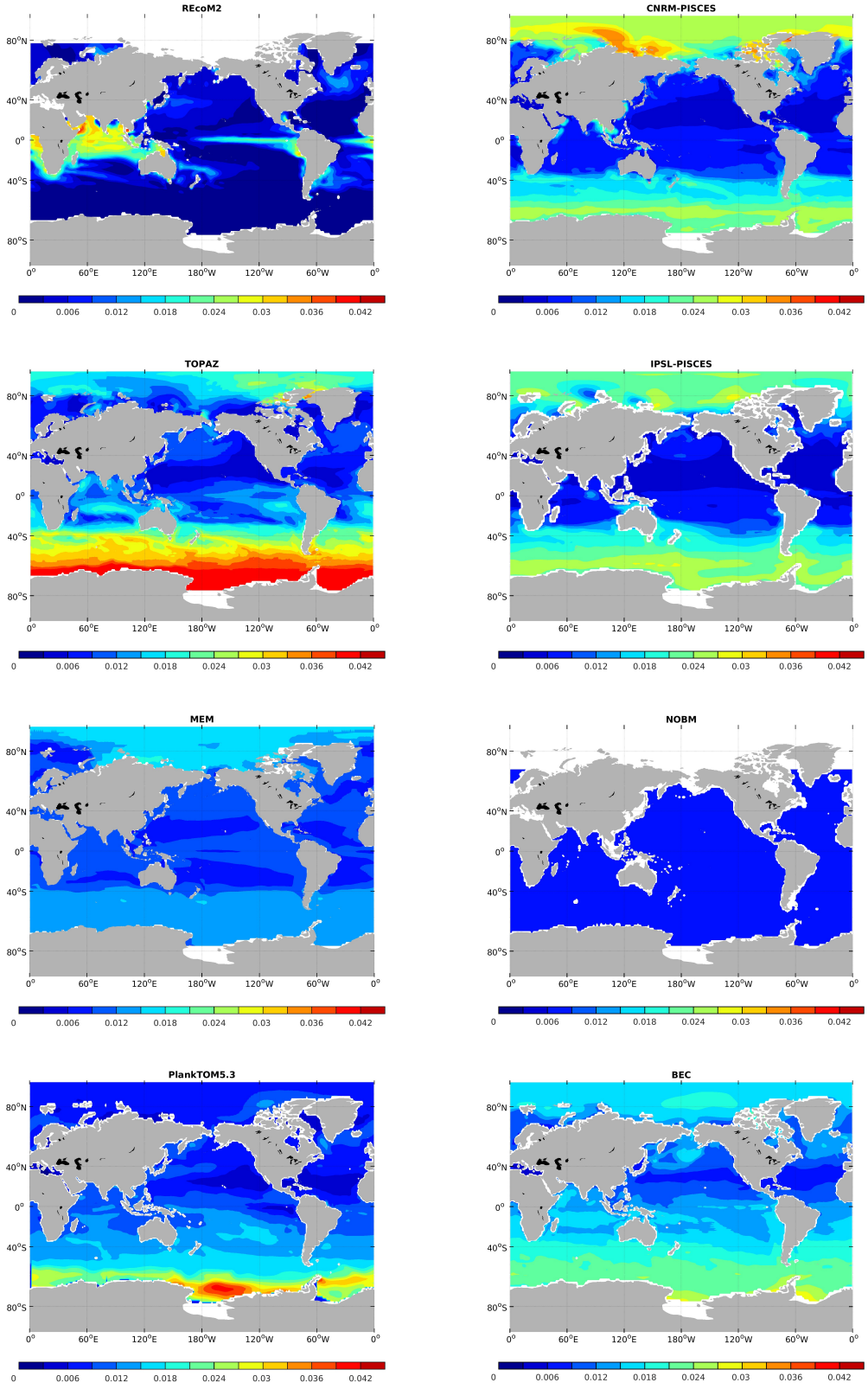

Appendix G: Latitudinal behaviour of the C:Chl ratio

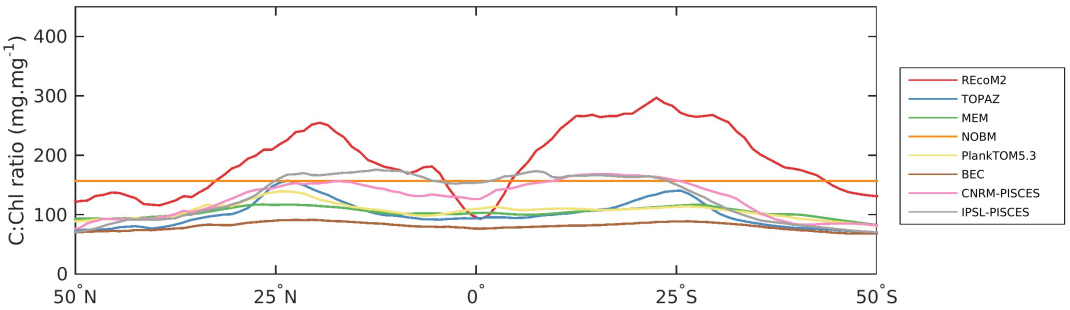

Annual climatology of averaged C:Chl ratio (mg mg^{-1}) as a function of latitude in surface waters from model simulations

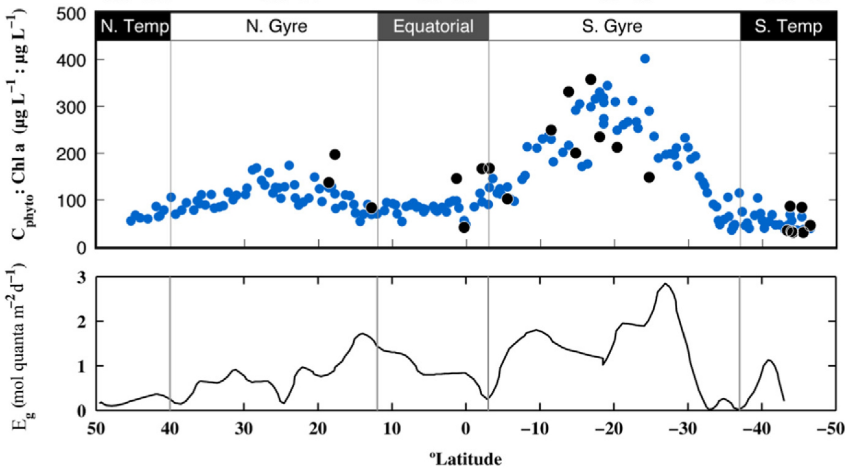

"Transect data from AMT-22 for C_{phyto}:Chl a ratios from direct measurements of C_{phyto} (black circles) and optically derived from $b_{bp\ 470}$ (blue circles) [...]", from Graff et al. (2015). Lower panel kept for axis.

Appendix H: Annual climatology of C versus Chl in surface waters from model simulations. The regression line of the log-transformed variables is represented by the black line. Equation 15 is represented by the red line and Equation 16 by the orange line.

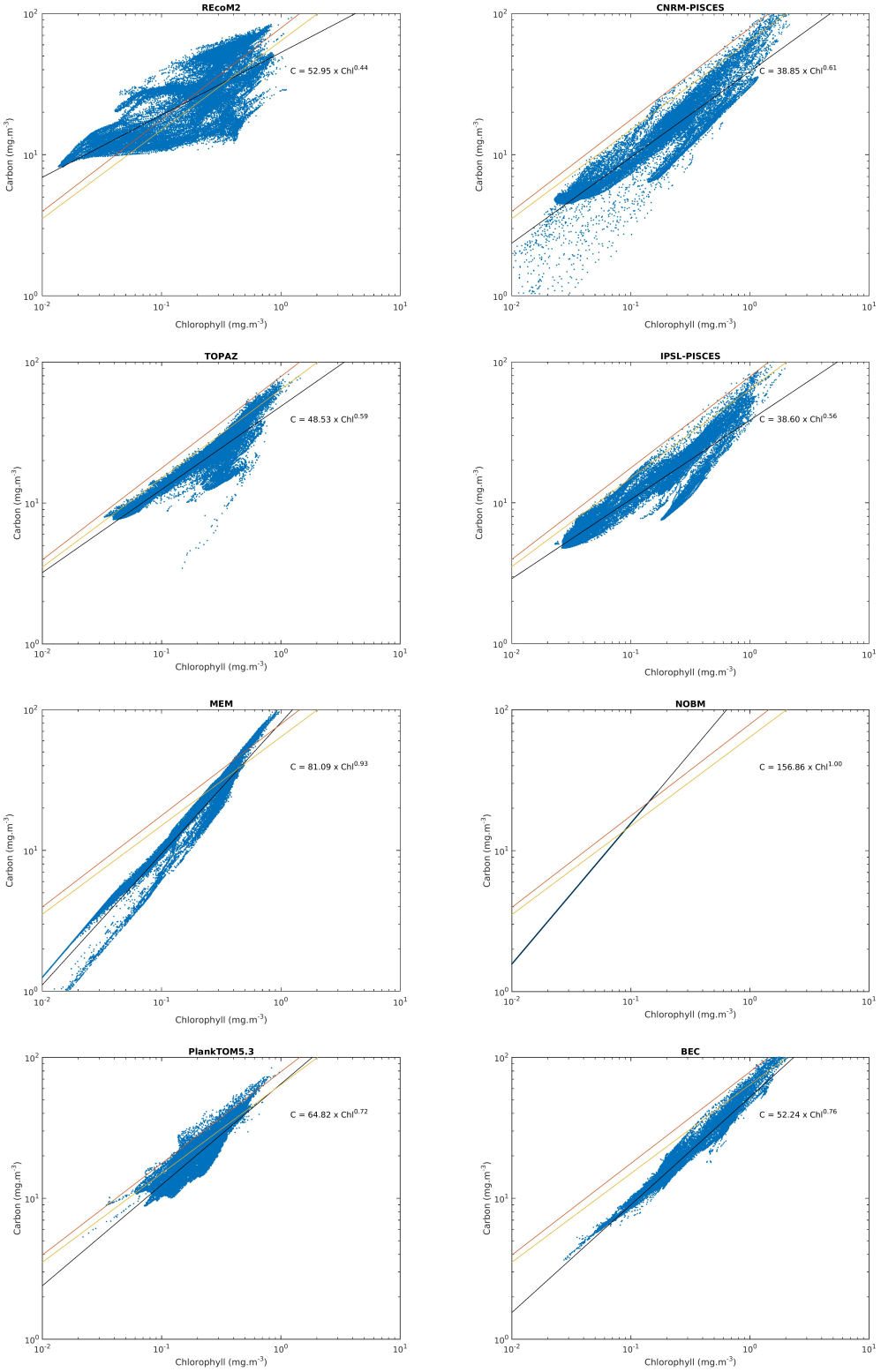

Appendix I: Distribution of the dominant limiting nutrient for diatoms in surface waters from model simulations. The legend being Blue=N limitation, Cyan=P limitation, Yellow=Si limitation, Red=Fe limitation, Dark blue indicates that none of the nutrient limitation is lower than 0.7, so either there is no limitation, or it is light limited.

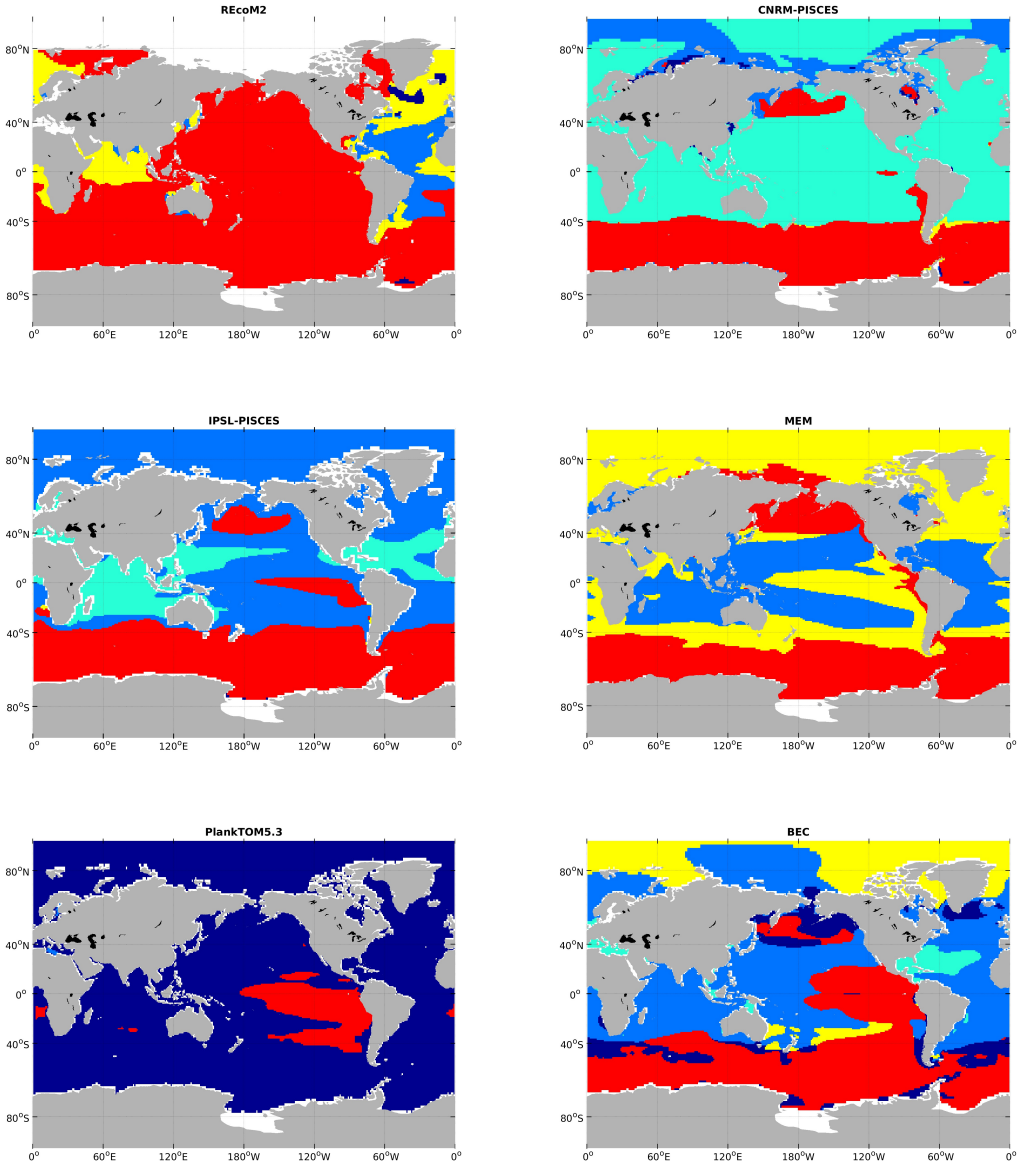

Appendix J: Distribution of the dominant limiting nutrient for nanophytoplankton in surface waters from model simulations. The legend being Blue=N limitation, Cyan=P limitation, Red=Fe limitation, Dark blue indicates that none of the nutrient limitation is lower than 0.7, so either there is no limitation, or it is light limited.

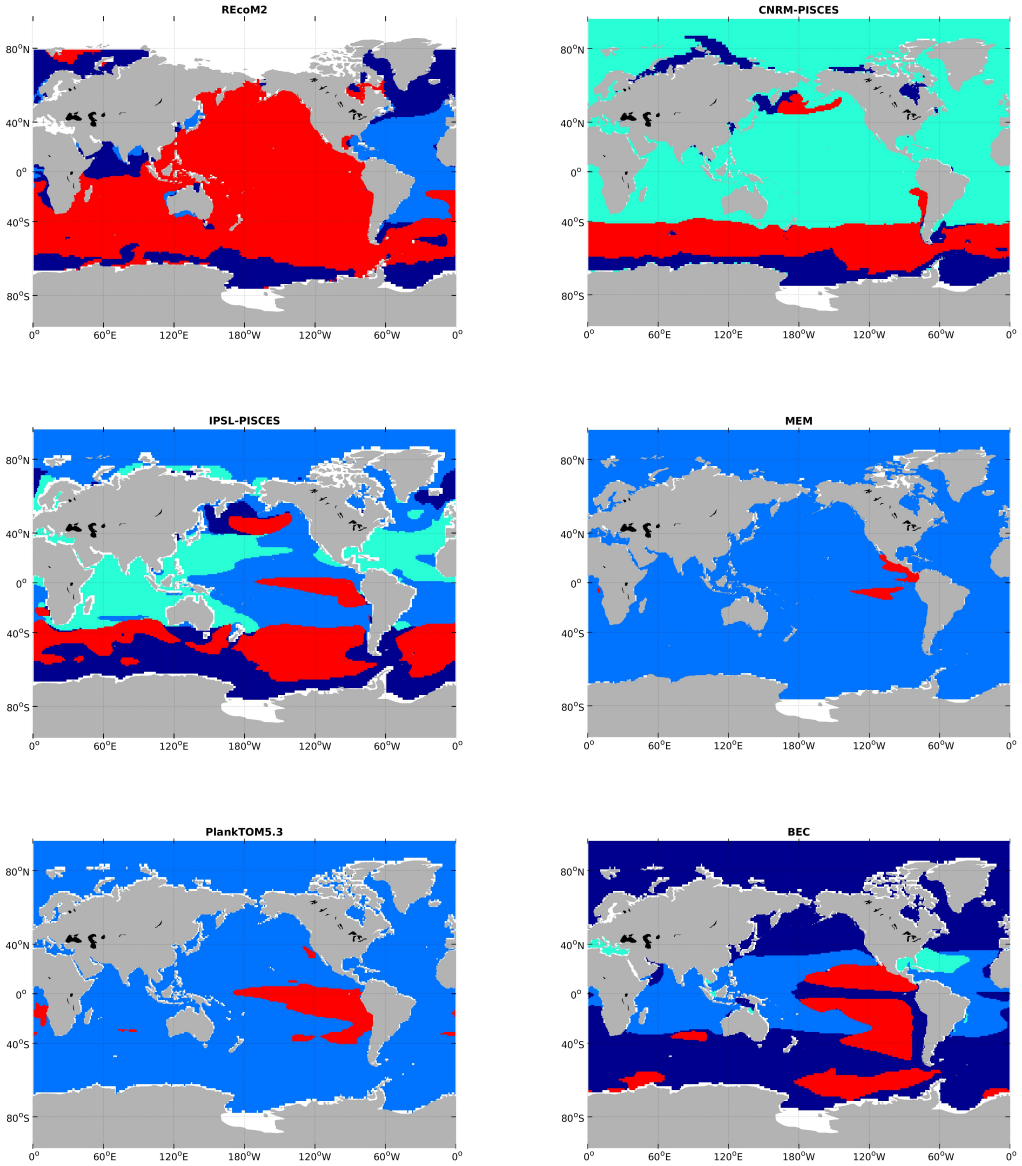

Appendix K: January and July climatologies of the relative change of C for diatoms and nanophytoplankton in surface waters simulated by REcoM2.

Diatoms

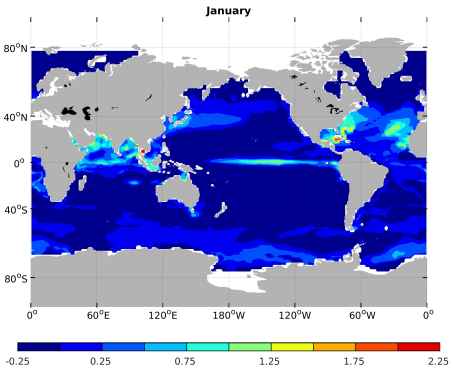

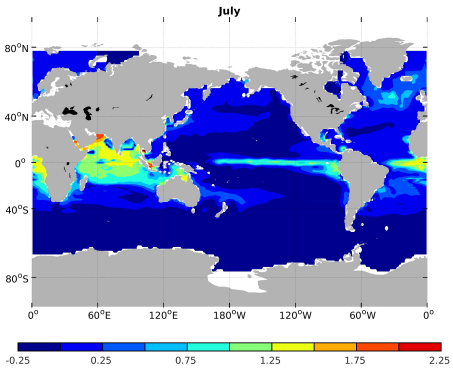

Nanophytoplankton

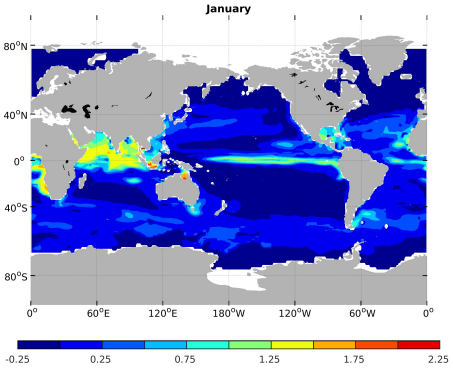

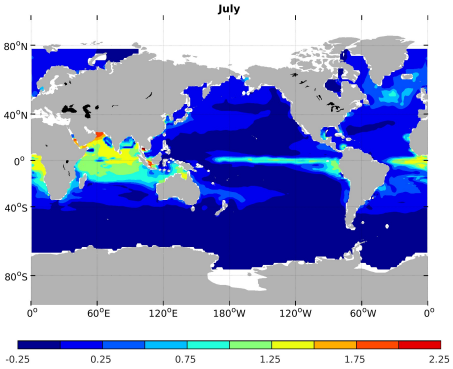

Appendix L: Initial model run and sensitivity runs on the annual climatology of the Chl:C ratio (mg mg^{-1}) in surface waters for diatoms and nanophytoplankton in REcoM2. Note that the scale was kept similar to the one in Figure 8 to facilitate comparison.

Diatoms

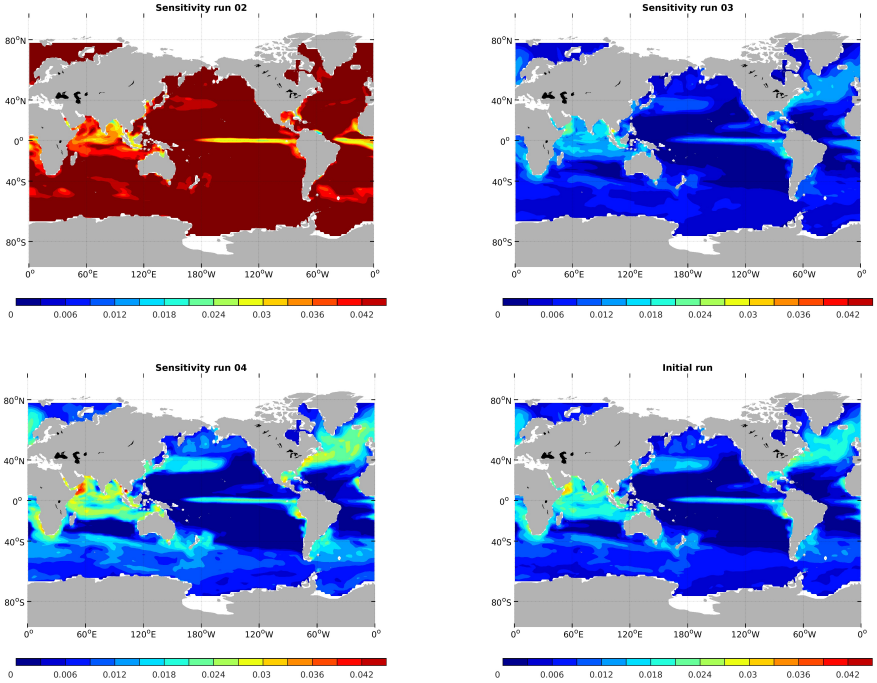

Nanophytoplankton

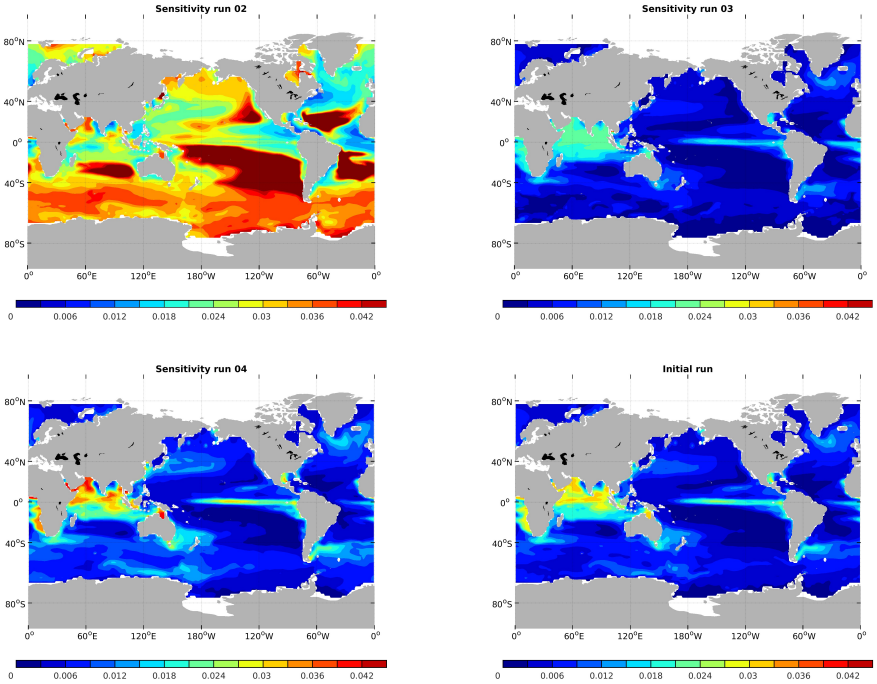

université de BORDEAUX

UNIVERSITY OF Southampton

eman ta zabal zazu
Universidad del País Vasco
Euskal Herriko Unibertsitatea

Université de Liège